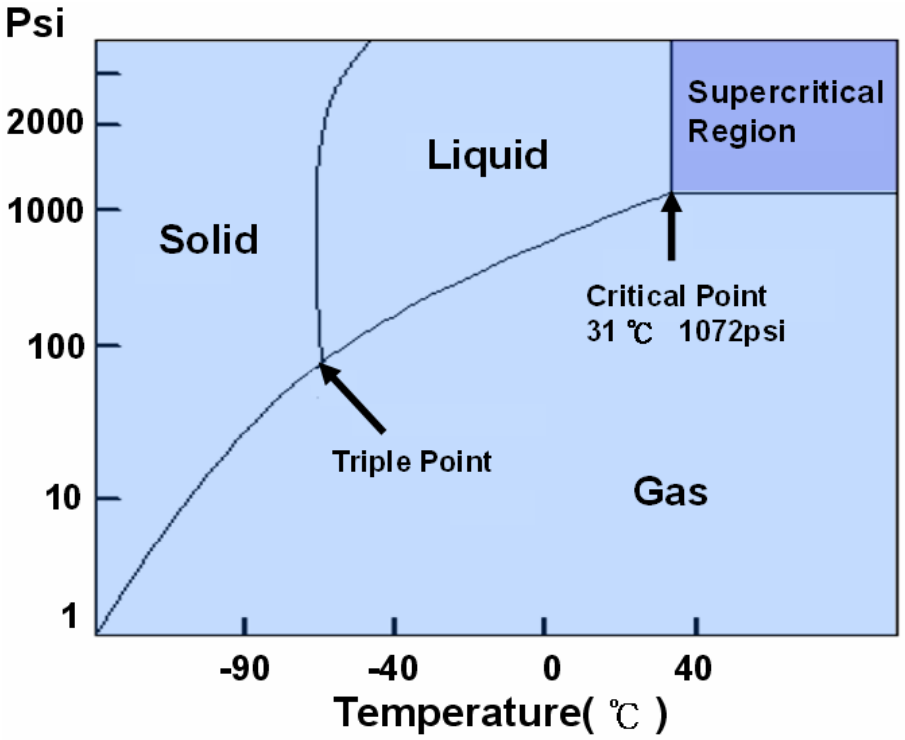

Fig. 1-1 Phase diagram for CO_2.

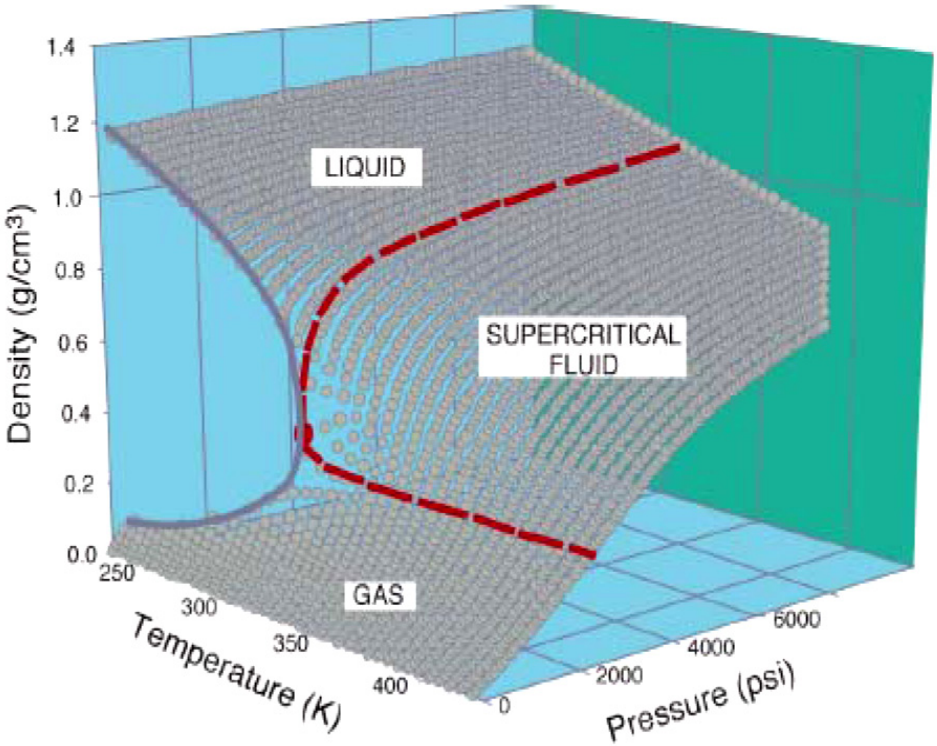

Fig. 1-2 Density-pressure-temperature surface for pure CO_2.

Fluid	Critical Temperature(℃)	Critical Pressure (Psi) (1atm=14.7psi)
Heliu (He)	-268	33
Neon (Ne)	-229	400
Argon (Ar)	-122	706
Nitrogen (N_2)	-147	492
Oxygen (O_2)	-119	731
Carbon dioxide (CO_2)	31	1072
Sulfur hexafluoride (SF_6)	46	545
Ammonia (NH_3)	133	1654
Water (H_2O)	374	3209

Table 1-1 Critical temperature and pressure for some common fluids.

	Liquid	Supercritical Fluid	Vapor
Density (g/cm^3)	1.0	0.3 ~ 0.7	~ 10^{-3}
Diffusivity (cm^2/sec)	< 10^{-5}	10^{-2} ~ 10^{-5}	~ 10^{-1}
Viscosity (g/cm-sec)	~ 10^{-2}	10^{-3} ~ 10^{-6}	~ 10^{-6}

Table 1-2 Comparison of physical properties of CO_2.

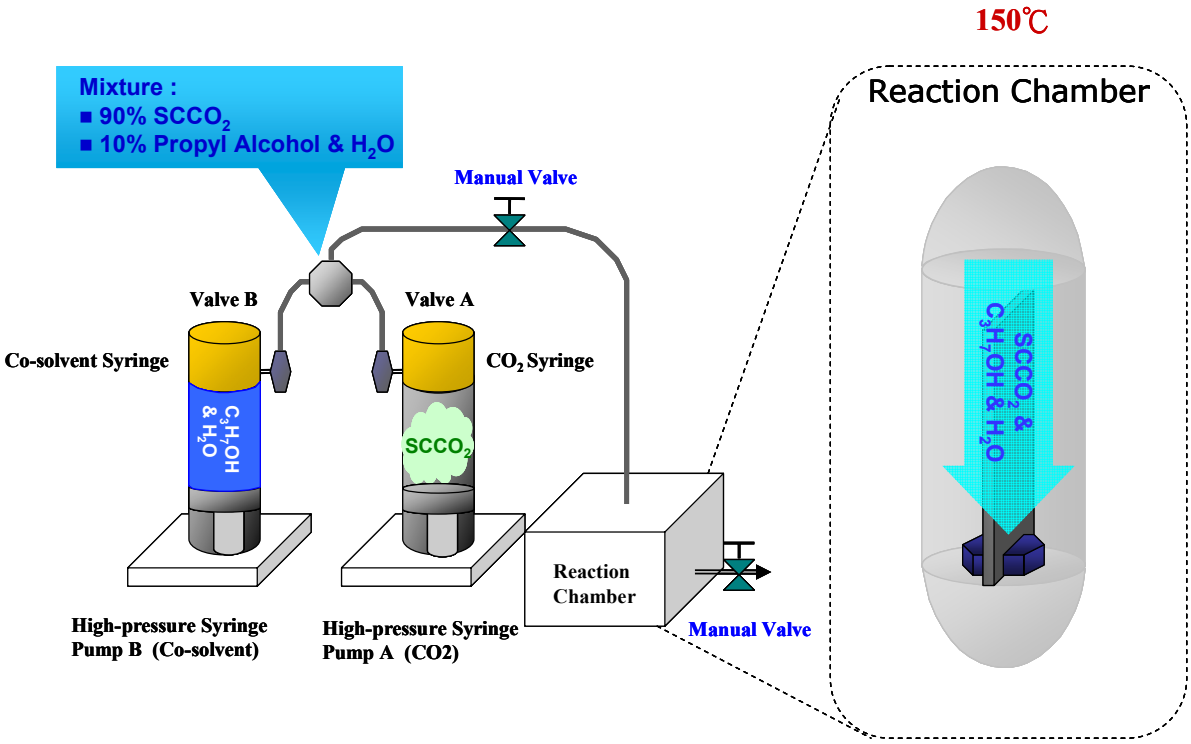

(a) $SCCO_2$ Treatment Process

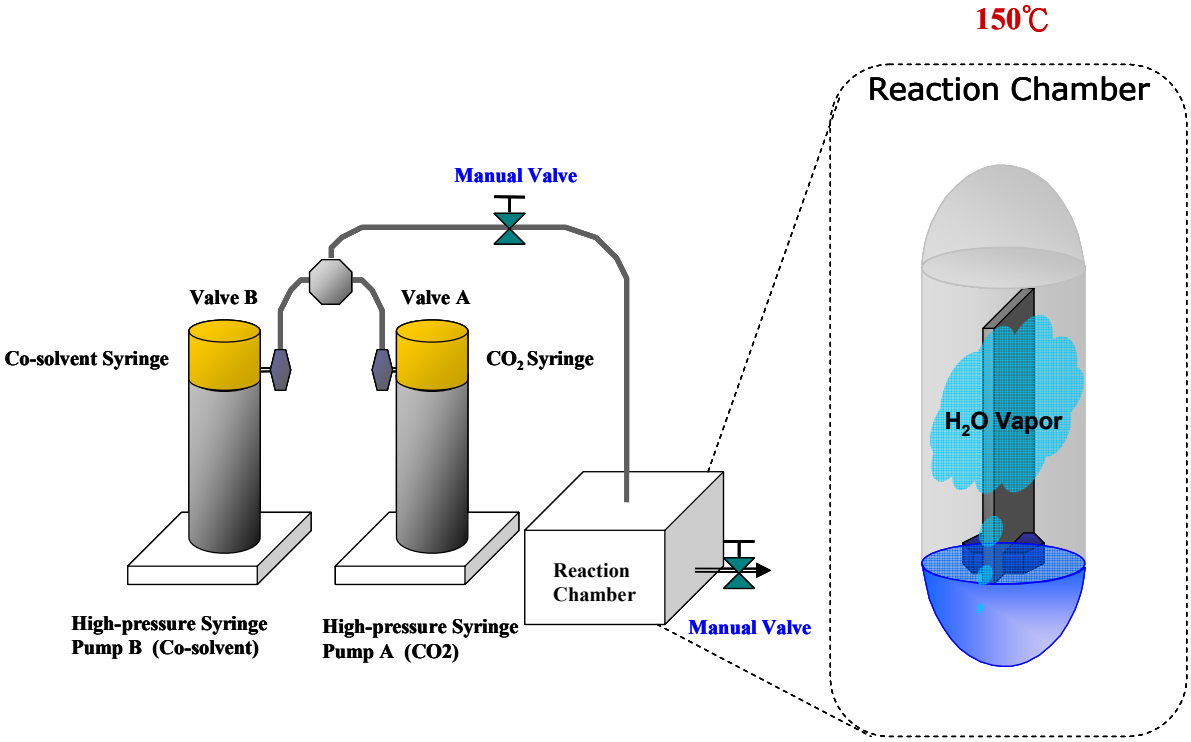

(b) H_2O-Vapor Treatment Process

Fig. 2-1 The supercritical fluid system.

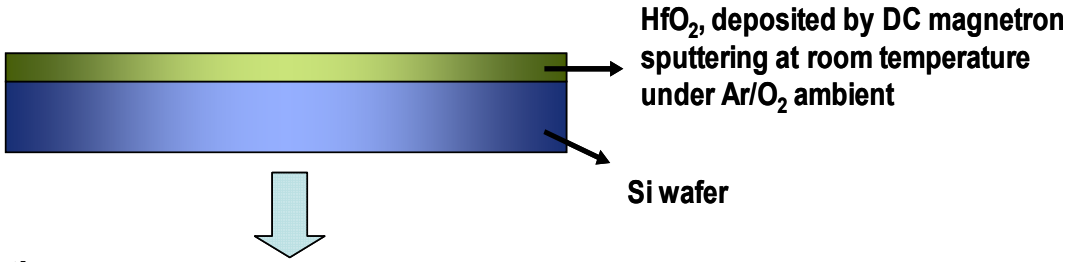

Defect passivation process:

1. ***Baking-only treatment***: only baked on a hot plate at 150 ˚C for 2 hrs.
2. ***H_2O vapor treatment***: immersed into a pure H_2O vapor ambience at 150 ˚C for 2 hrs.
3. ***1500~3000psi-$SCCO_2$ treatment***: was placed in the supercritical fluid system at 150˚C for 2 hrs.

Analysis of Material:

1. **Fourier transformation infrared spectroscopy (FTIR).**
2. **Thermal desorption spectroscopy (TDS).**
3. **X-ray Photoelectron Spectroscopy (XPS).**
4. **Auger Depth Profile (AES).**
5. **Transmission Electron Microscopy (TEM).**

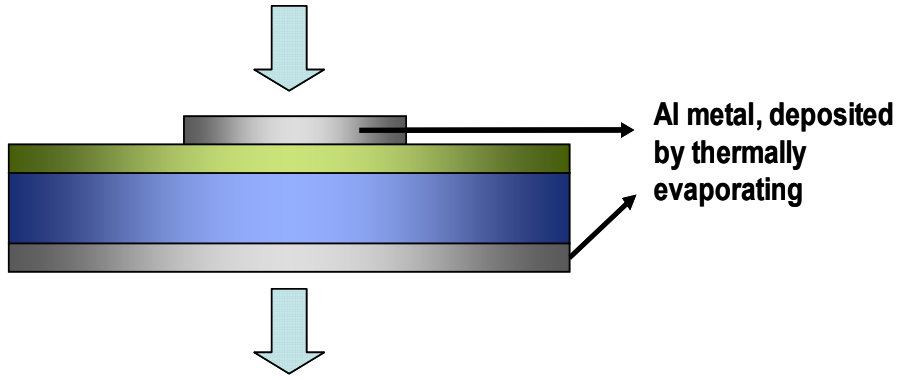

Analysis of Electrical characteristics:

1. **current density-electric field (J-E) characteristics.**
2. **capacitor-voltage (C-V) characteristics.**
3. **breakdown voltage**
4. **gate bias stress**

Fig. 2-2 The experiment processes of thin HfO_2 film with various treatments.

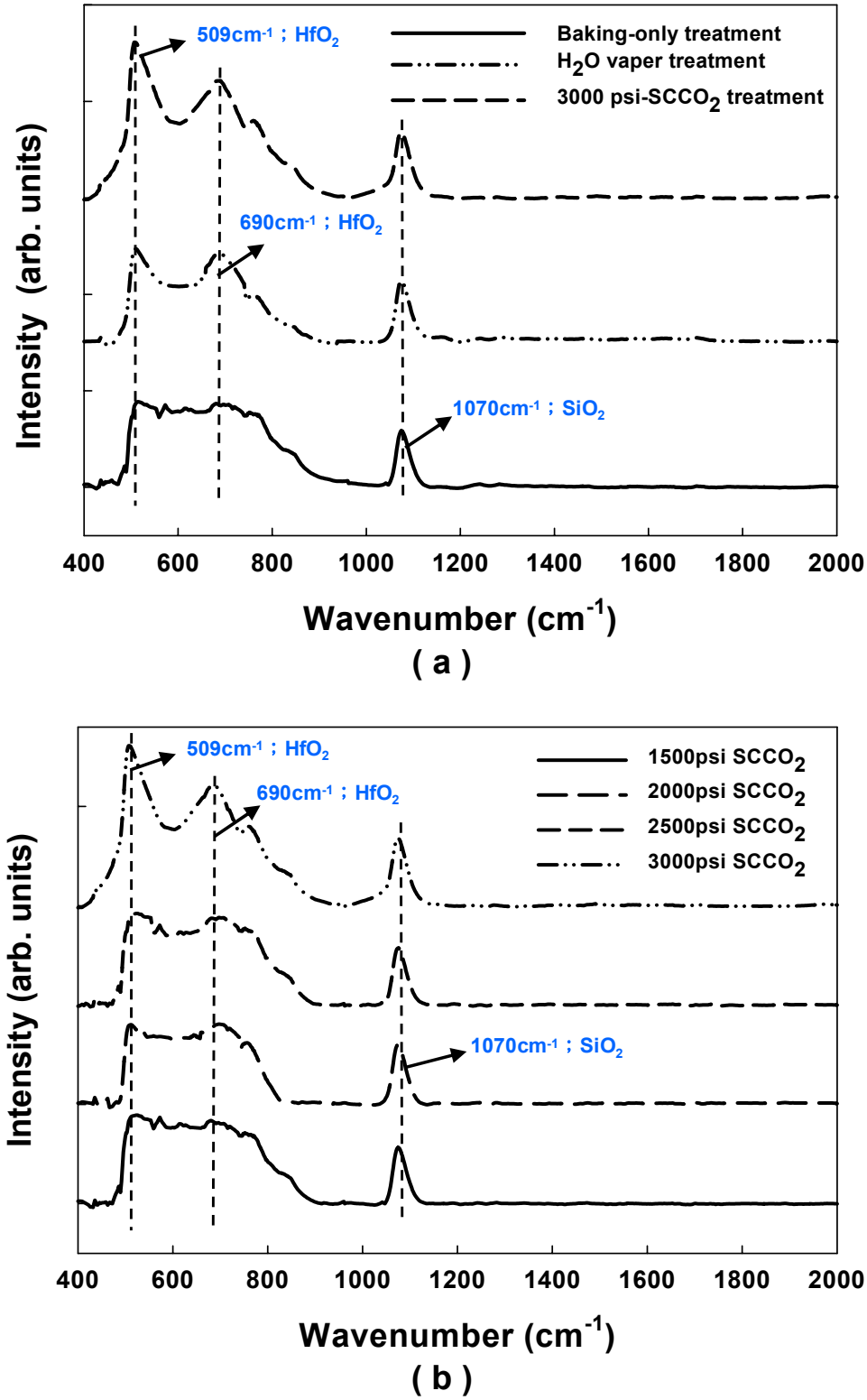

Fig. 2-3 The FTIR spectra of HfO_2 films (a) after various post-treatments, including Baking-only, H_2O vapor and 3000psi-$SCCO_2$ treatment, (b) after $SCCO_2$ treatment under different pressure.

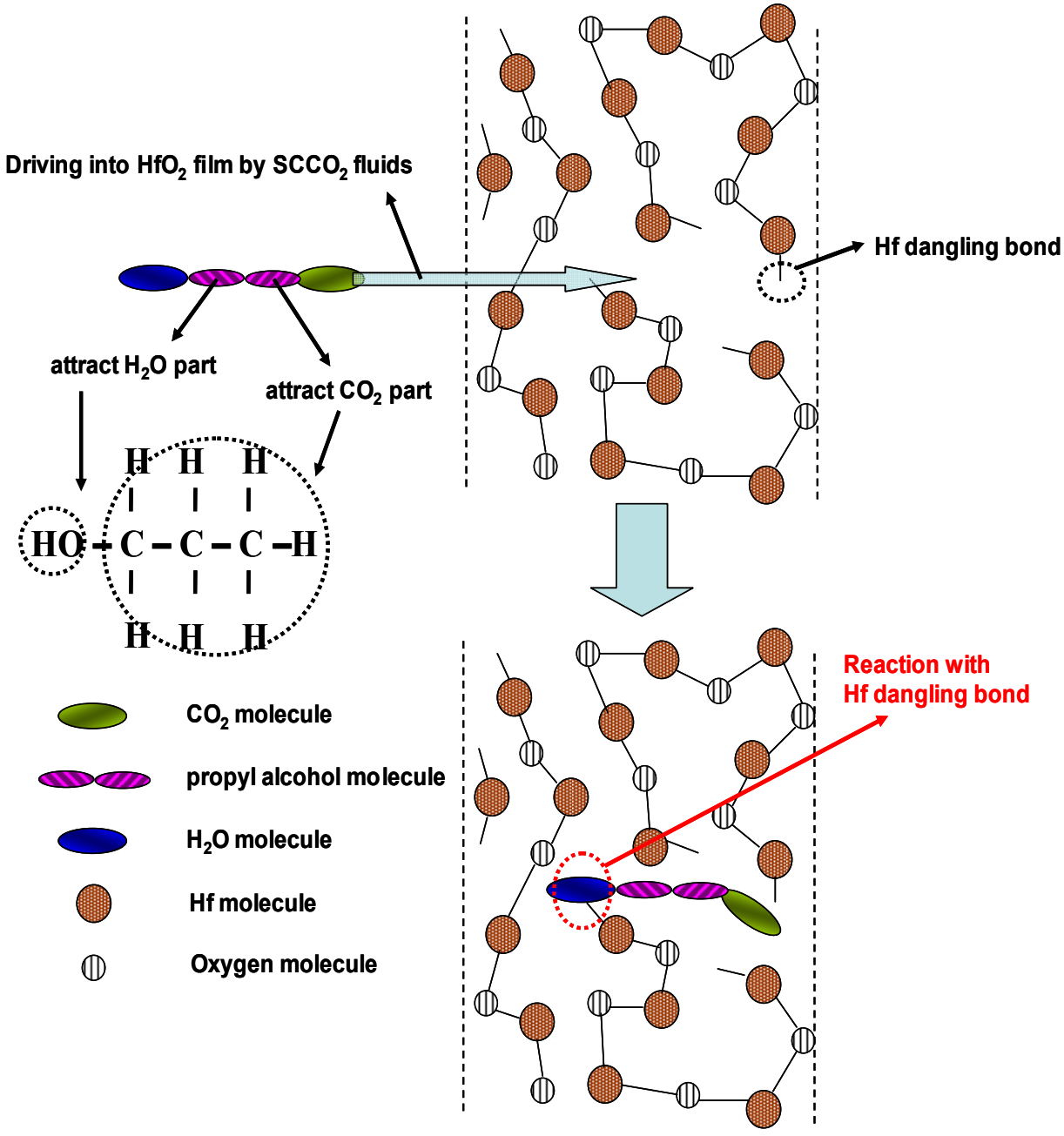

Fig. 2-4 The transporting mechanism for $SCCO_2$ fluids taking H_2O molecule into HfO_2 film.

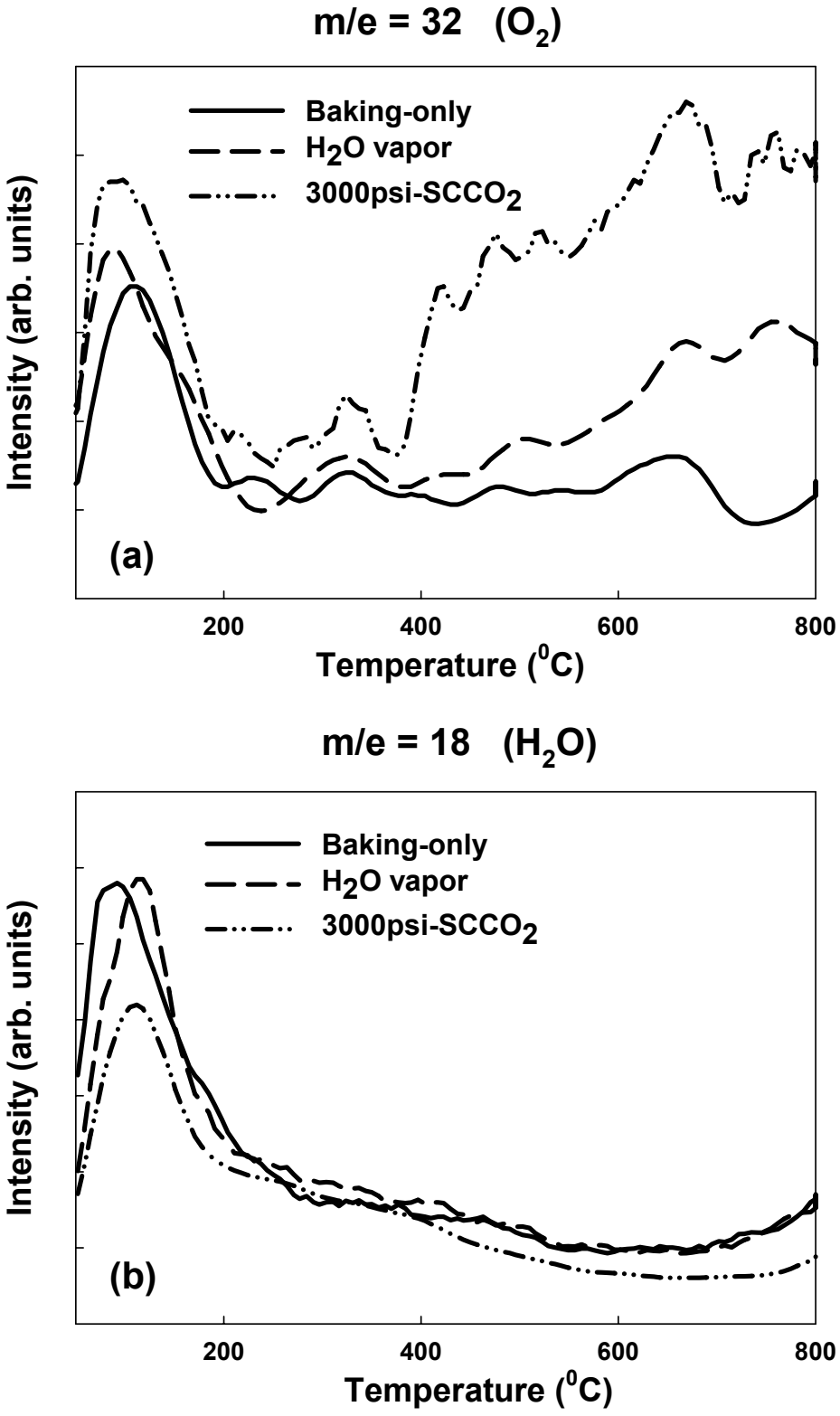

Fig. 2-5 The thermal desorption spectroscopy (TDS) measurement, (a) m/e (mass-to-charge ratio) = 32 peak that is attributed to O_2, (b) m/e = 18 peak that is attributed to H_2O.

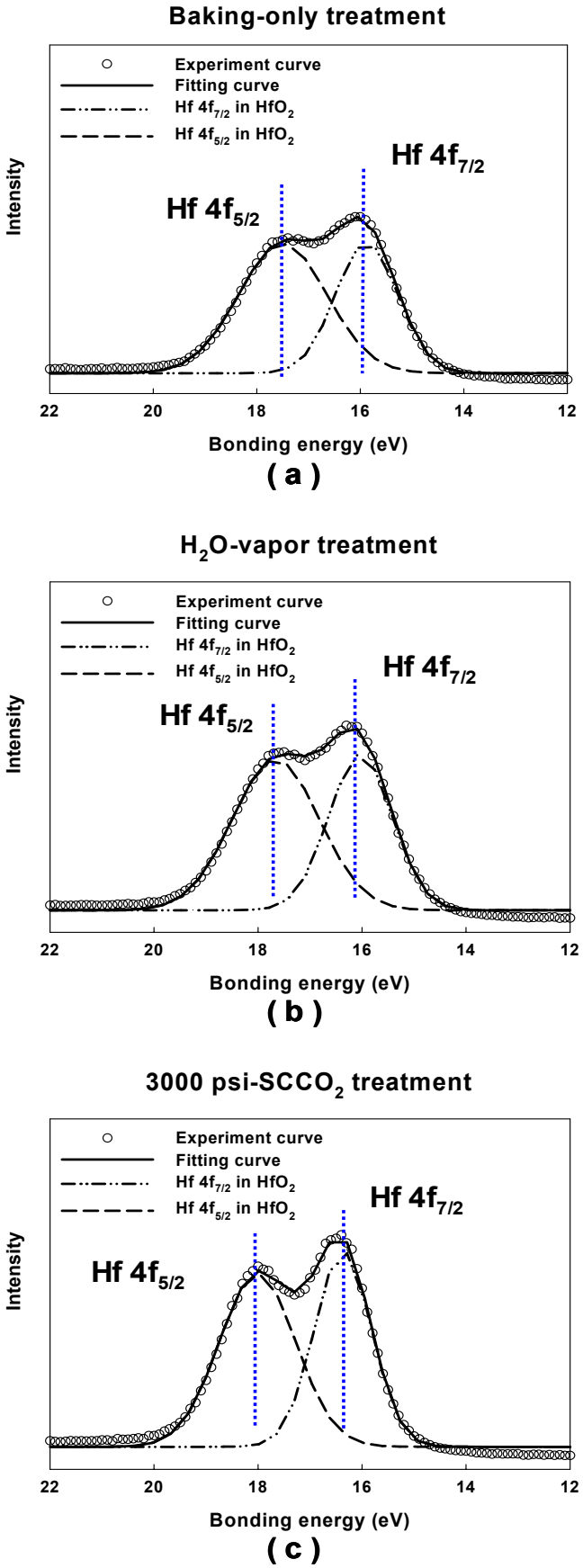

Fig. 2-6 The X-ray photoemission spectra of HfO_2 films Hf 4f after various post-treatments, including (a) Baking-only, (b) H_2O vapor and (c) 3000psi-$SCCO_2$ treatment.

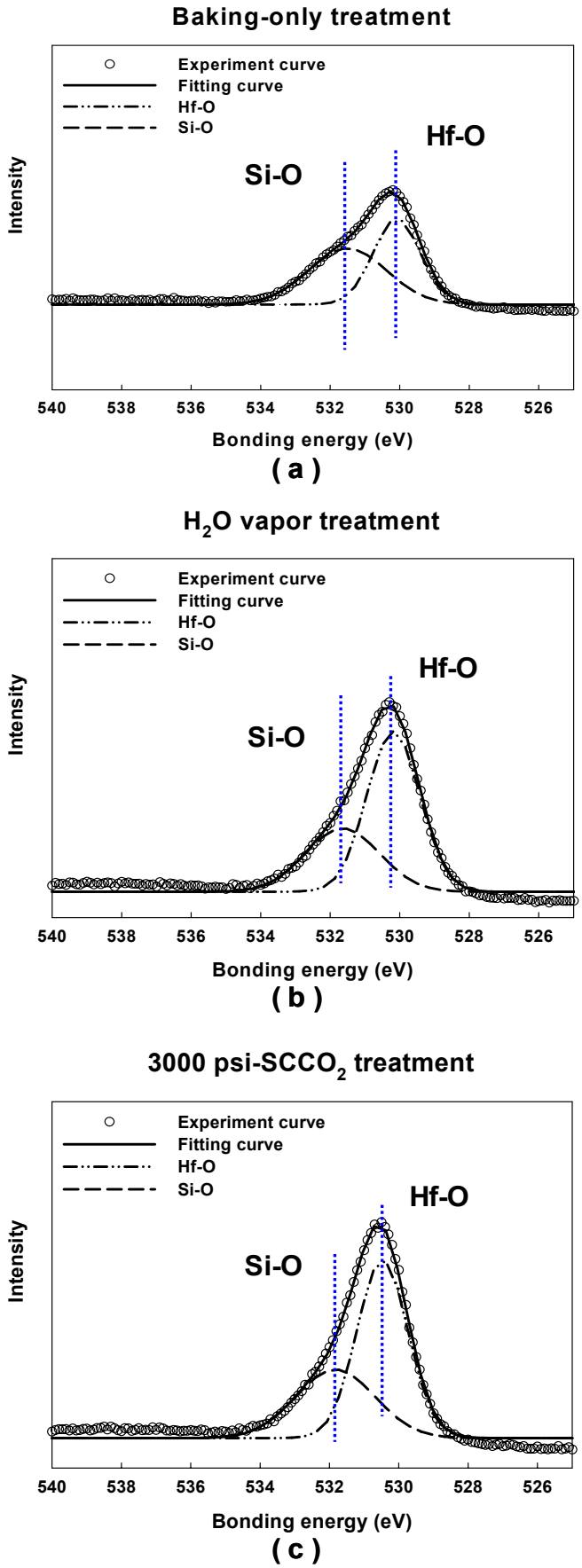

Fig. 2-7 The X-ray photoemission spectra of HfO_2 films O 1s after various post-treatments, including (a) Baking-only, (b) H_2O vapor and (c) 3000psi-$SCCO_2$ treatment.

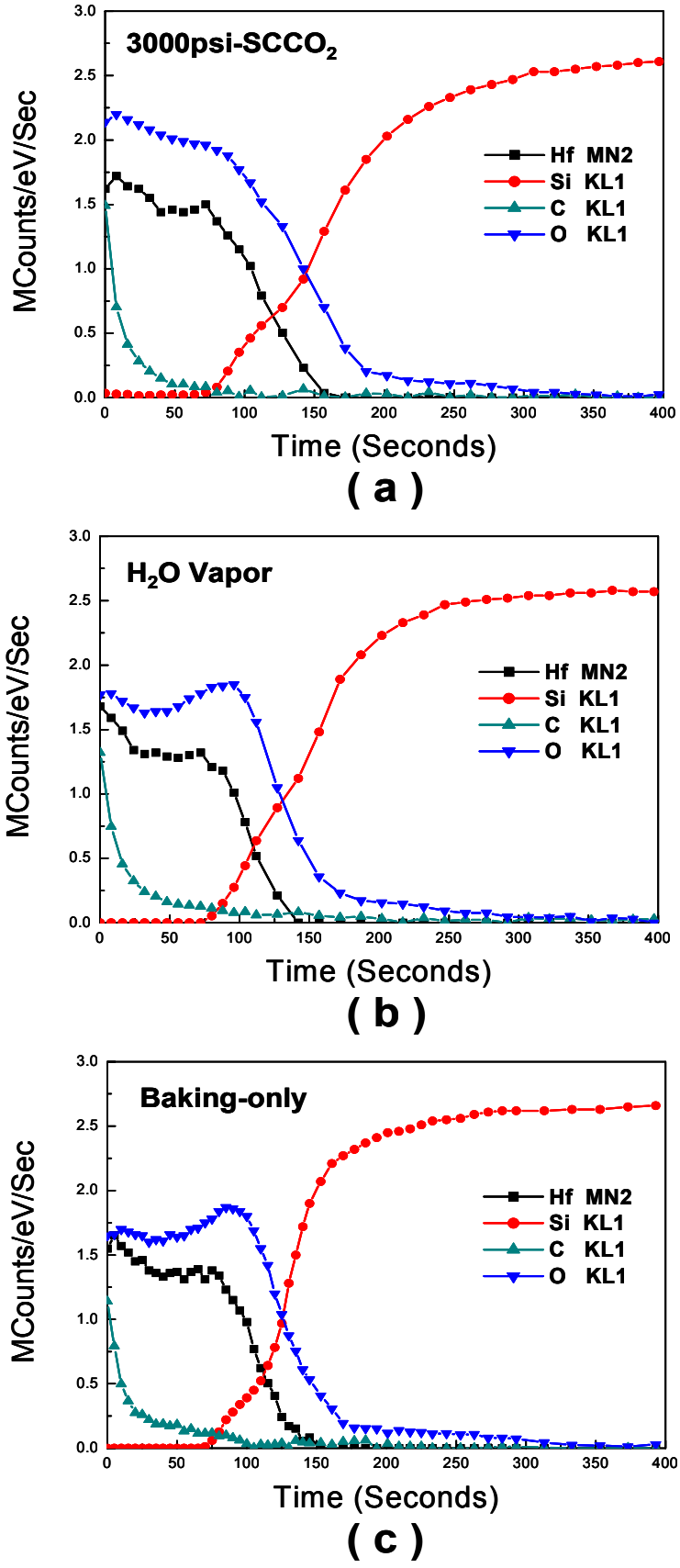

Fig. 2-8 Auger electron spectroscopy: (a) 3000psi-$SCCO_2$ treatment (b) H_2O vapor treatment and (c) Baking-only treatment.

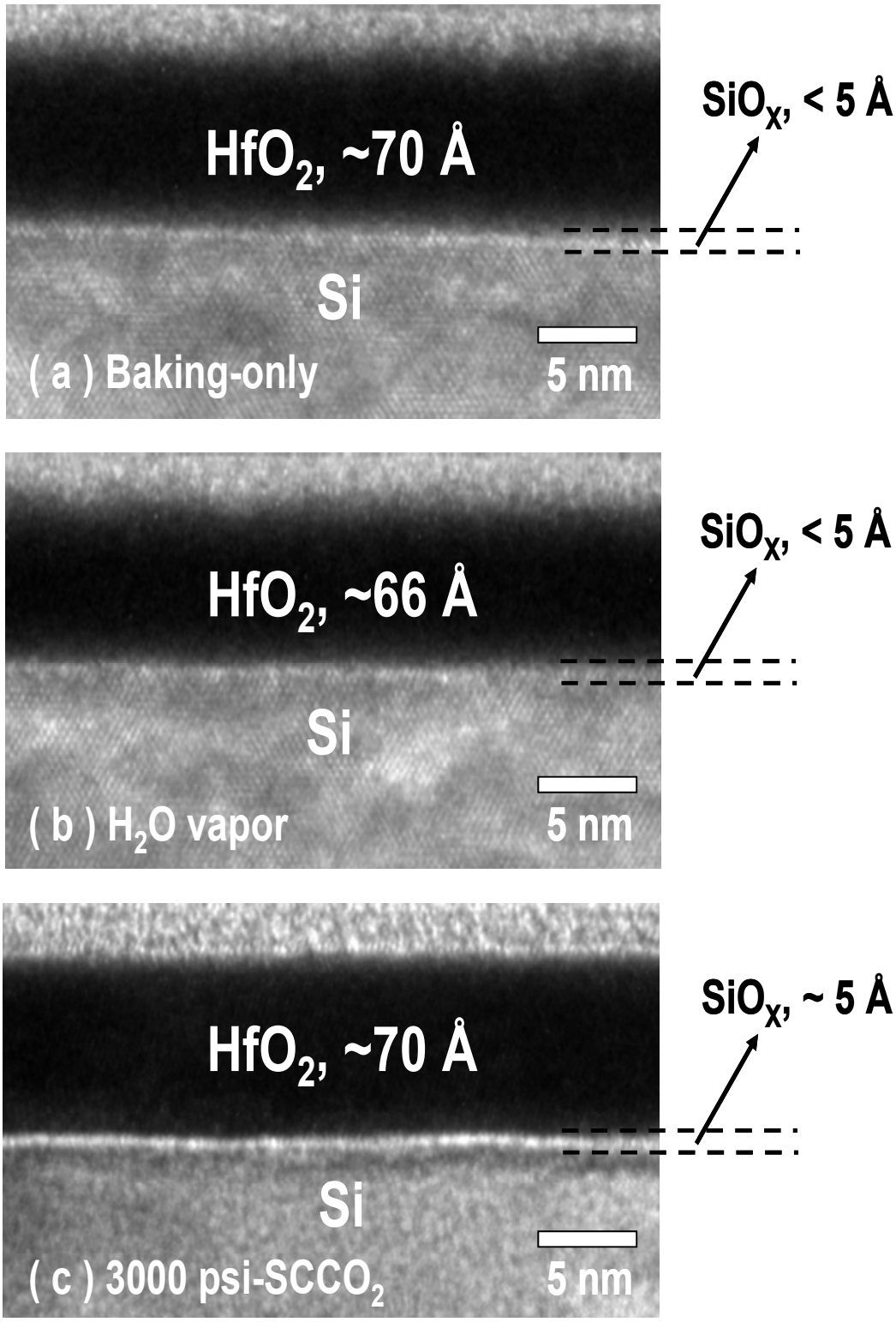

Fig. 2-9 The TEM images show the MIS ($Al/HfO_2/Si$-Substrate) structure after various post-treatments: (a) Baking-only treatment (b) H_2O vapor treatment and (c) 3000psi-$SCCO_2$ treatment.

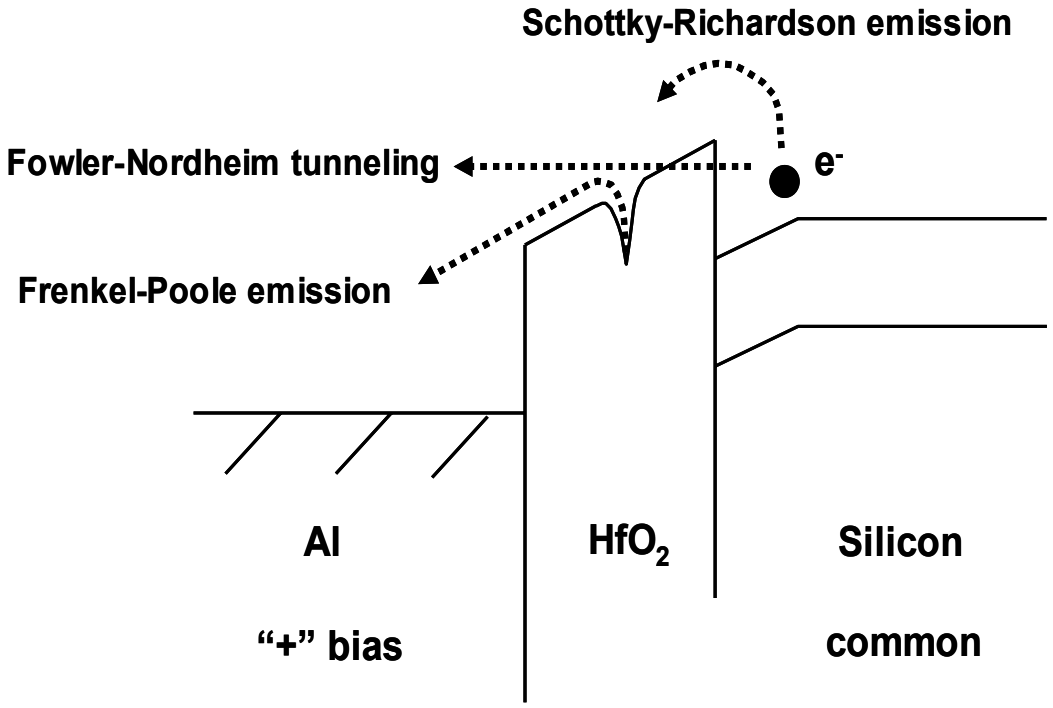

Fig. 2-10 Conduction mechanism for Al/HfO_2/Si MIS structure.

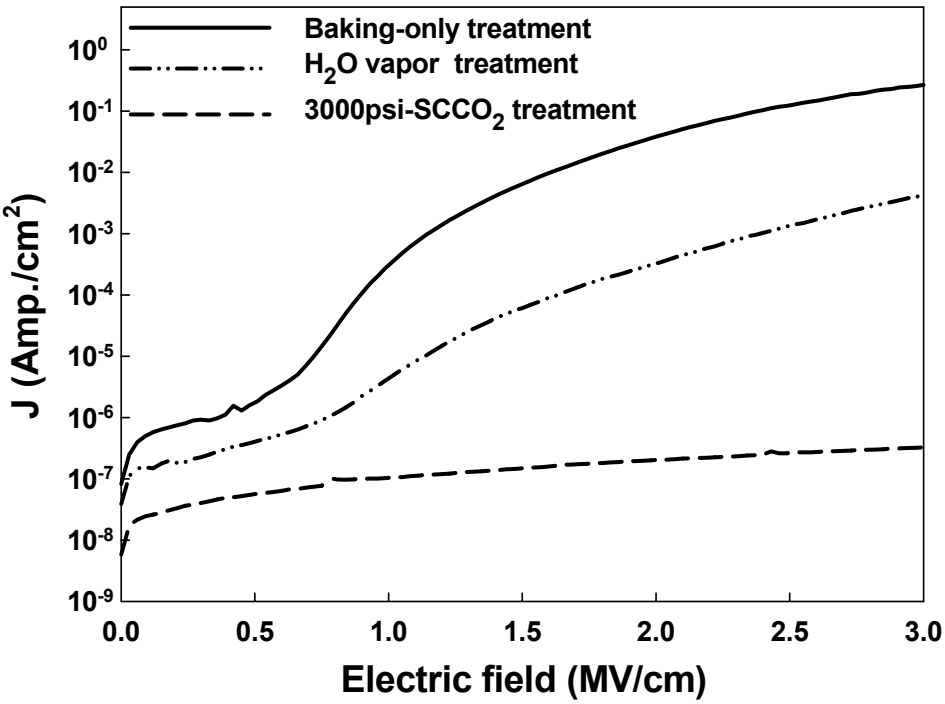

Fig. 2-11 The leakage current densities of HfO_2 films after different treatments. (The negative bias is applied on gate electrode)

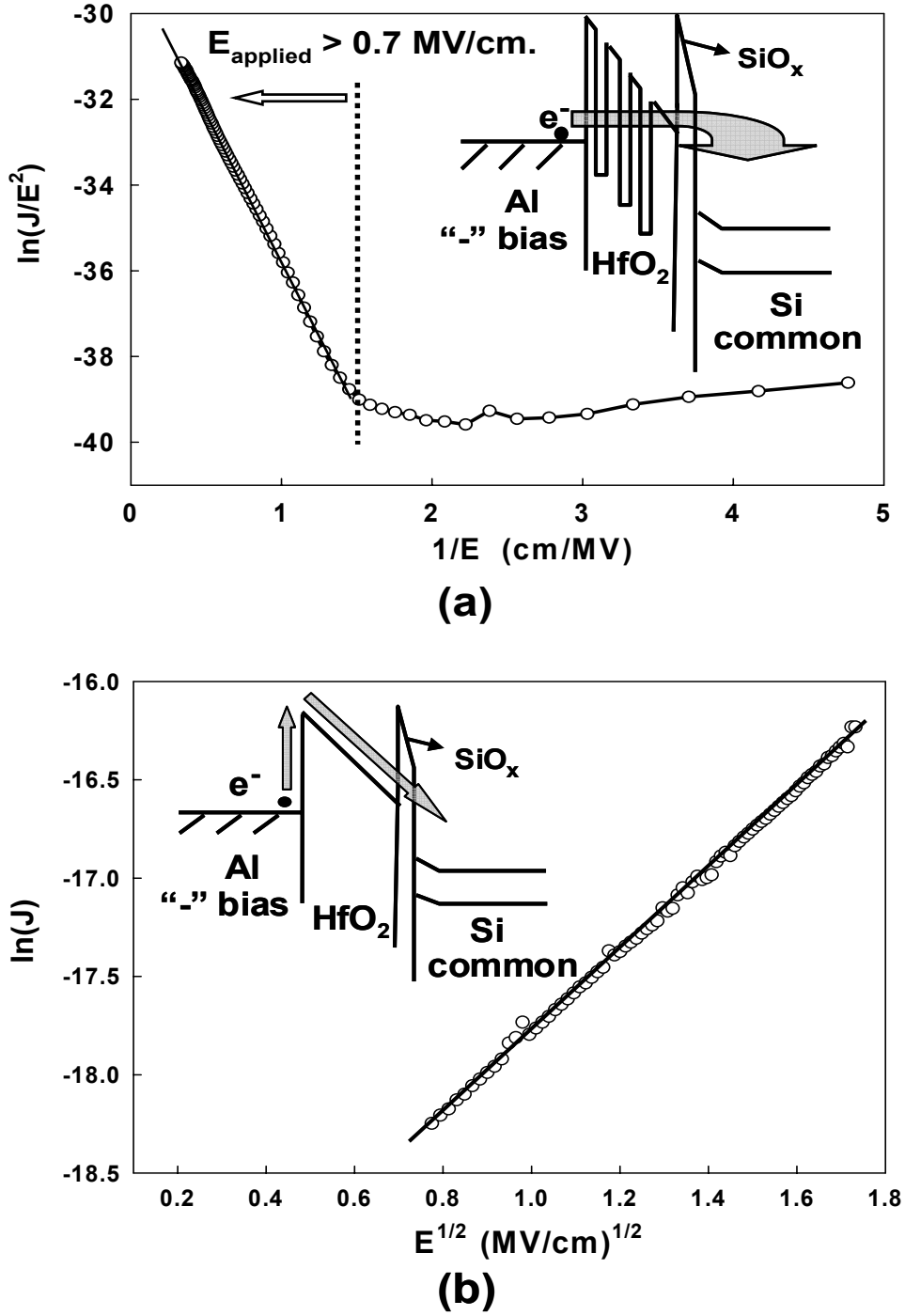

Fig. 2-12 (a) Curve of ln (J/E) versus reciprocal of electric field (*1/E*) for the baking-only treated HfO_2 film, and a schematic energy band diagram accounting for trap-assisted tunneling shown in the inset. (b) Leakage current density versus the square root of electric field ($E^{1/2}$) plot for the 3000 psi-$SCCO_2$ treated HfO_2 film. The inset shows the energy band diagram of Schottky-type conduction mechanism.

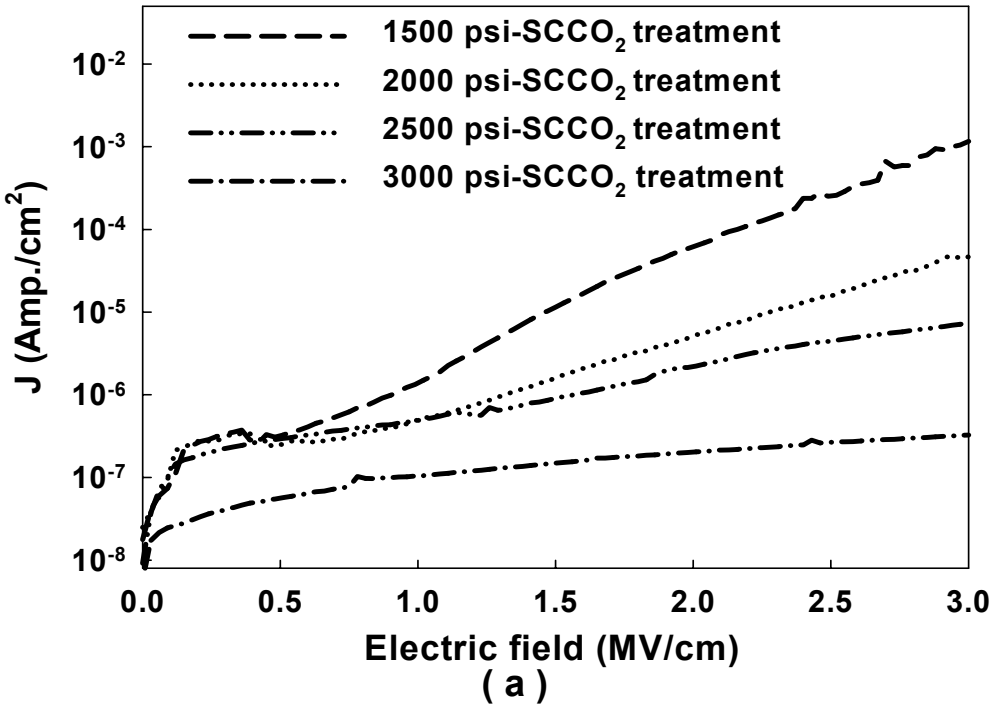

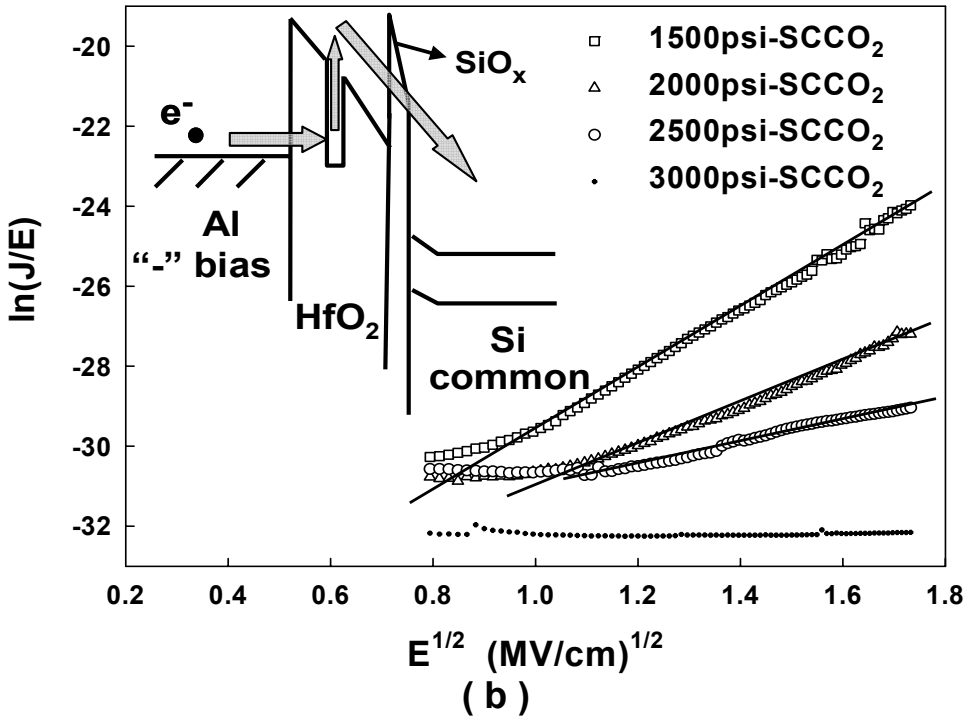

Fig. 2-13 (a) The leakage current densities of HfO_2 films after $SCCO_2$ treatments under different pressures (The negative bias is applied on gate electrode). (b) The plot of ln (J/E) versus $E^{1/2}$, which is according to Poole-Frenkel emission, and inset is the energy band diagram of Poole-Frenkel emission.

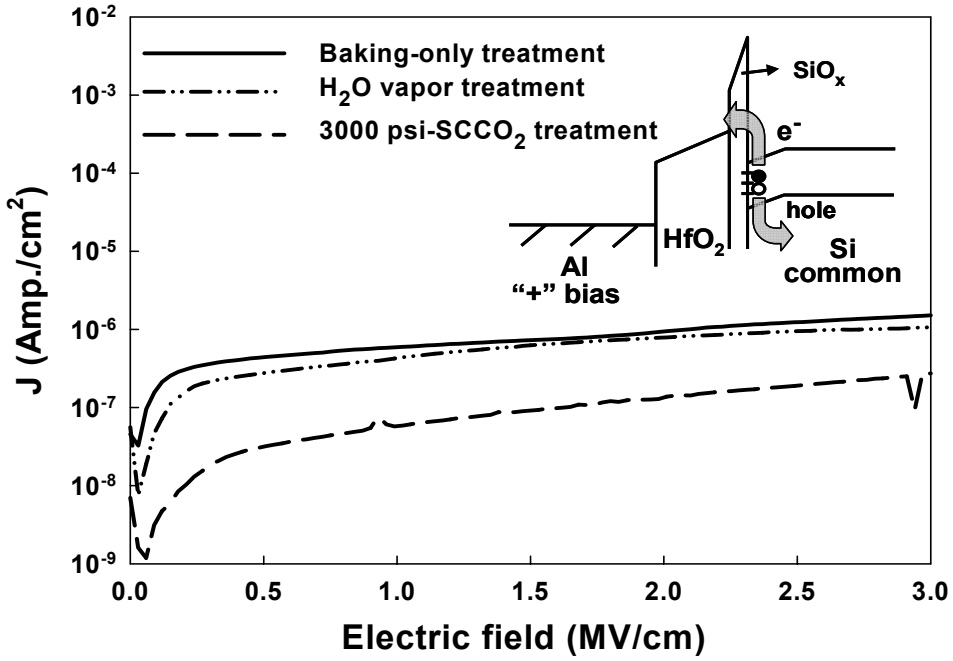

Fig. 2-14 The leakage current densities of HfO_2 films after different treatments (The positive bias is applied on gate electrode). Inset plots the energy band diagram of leakage current.

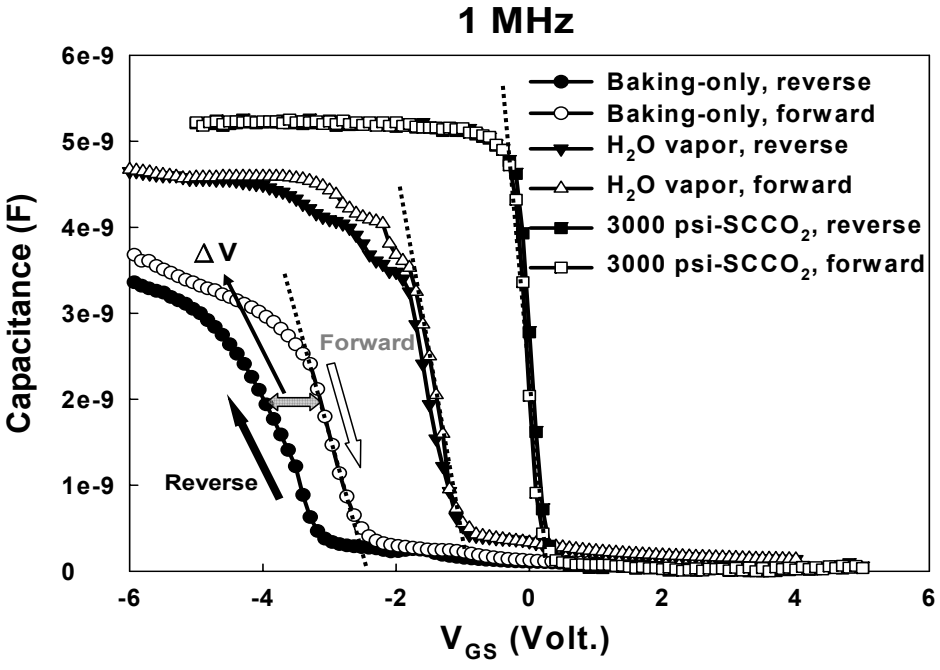

Fig. 2-15 The capacitance-voltage characteristics of HfO_2 films after different treatment, measuring at 1M Hz with gate bias swing from negative voltage to positive voltage (forward) and from positive voltage to negative voltage (reverse).

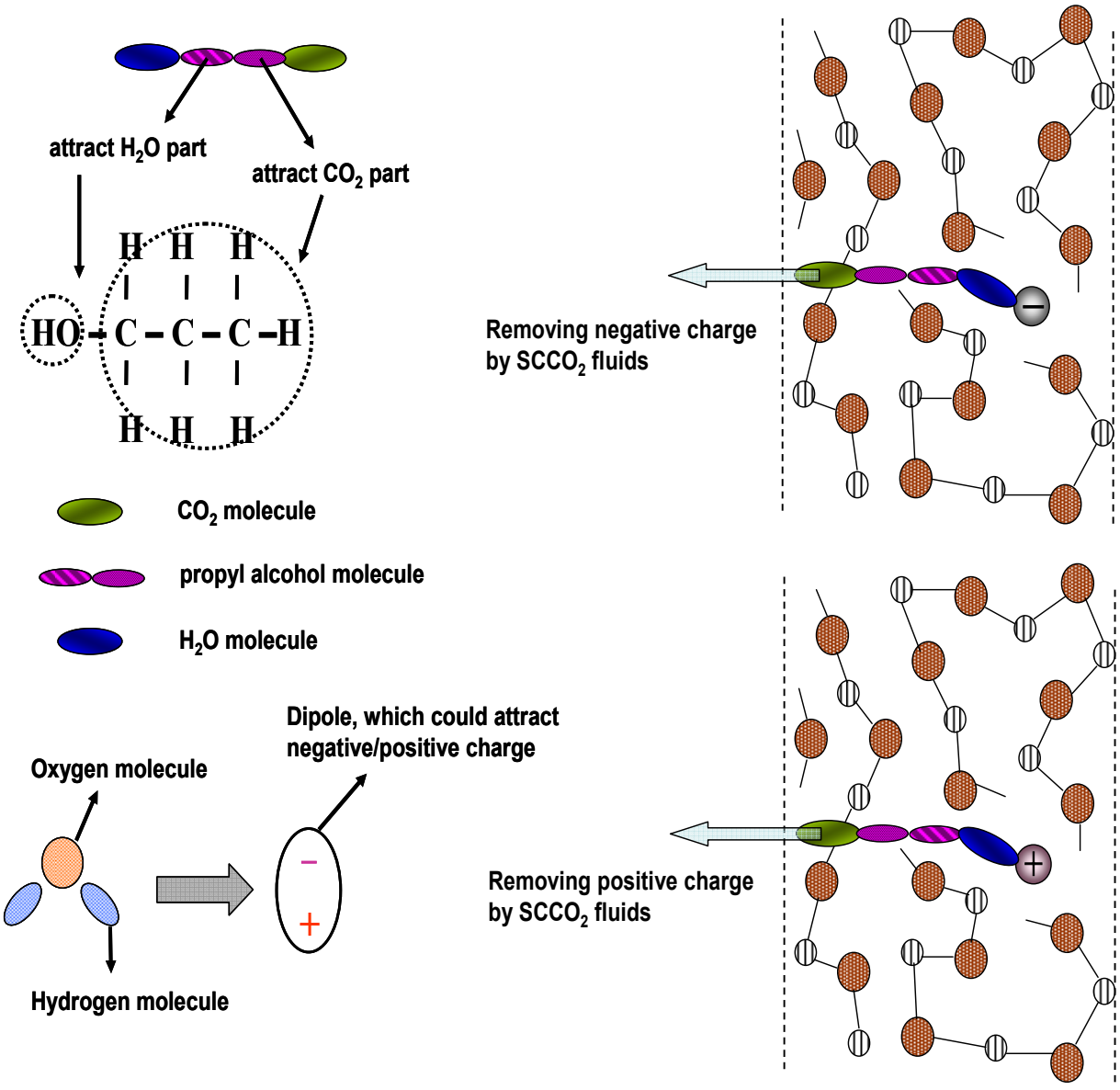

Fig. 2-16 The mechanism of extracting of fixed charge with $SCCO_2$ fluids.

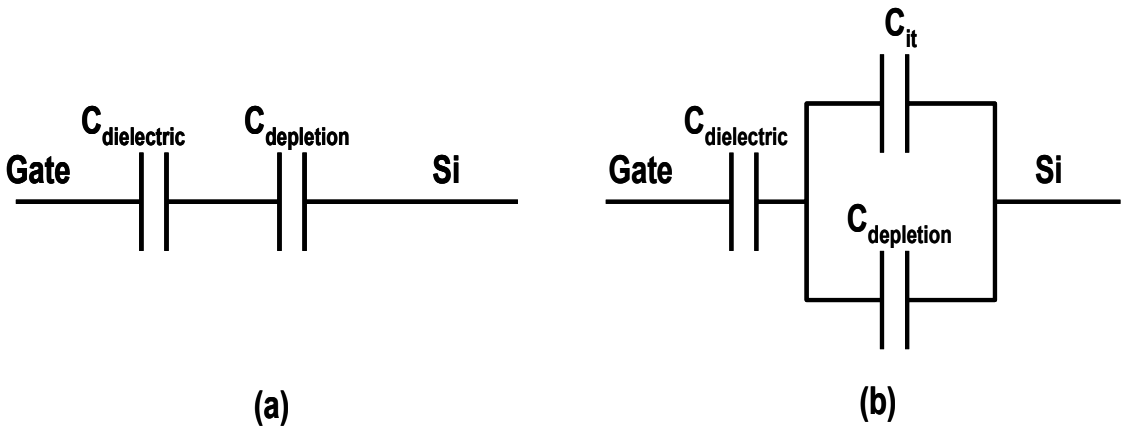

Fig. 2-17 The equivalent capacitance models of MOS structure (a) without C_{it}, (b) with C_{it}.

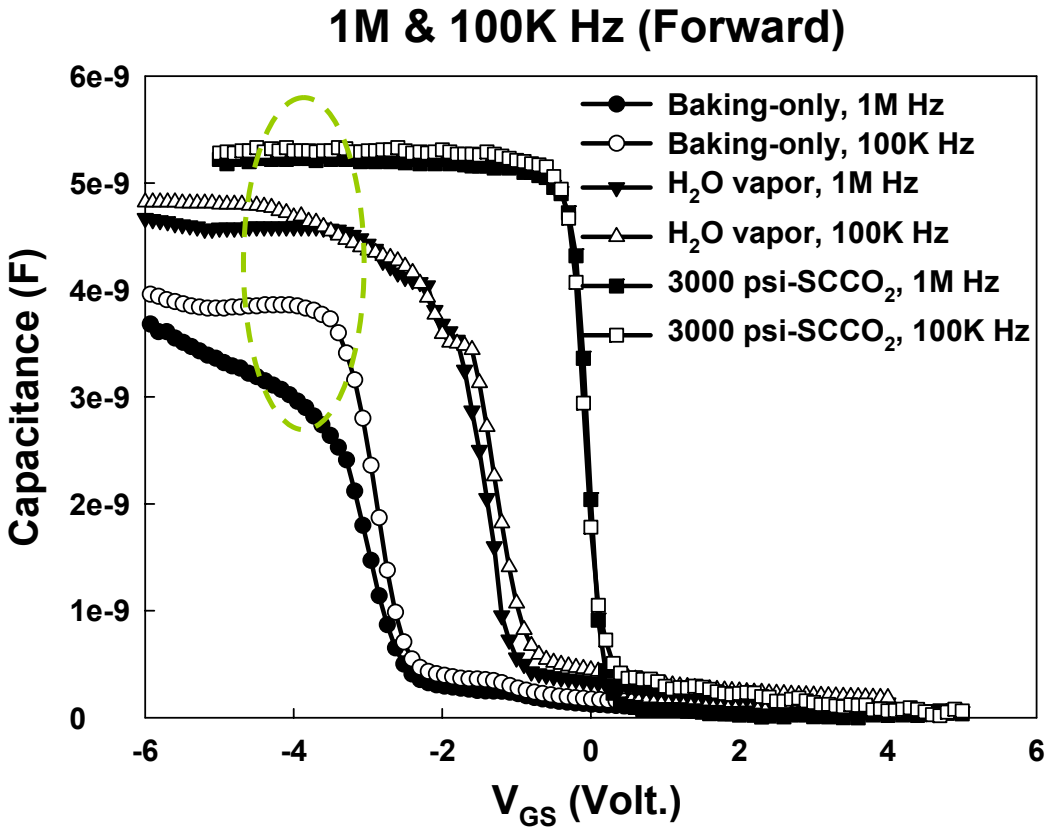

Fig. 2-18 The capacitance-voltage characteristics of HfO_2 films after different treatment, measuring at 1M Hz and 100k Hz with forward gate bias swing.

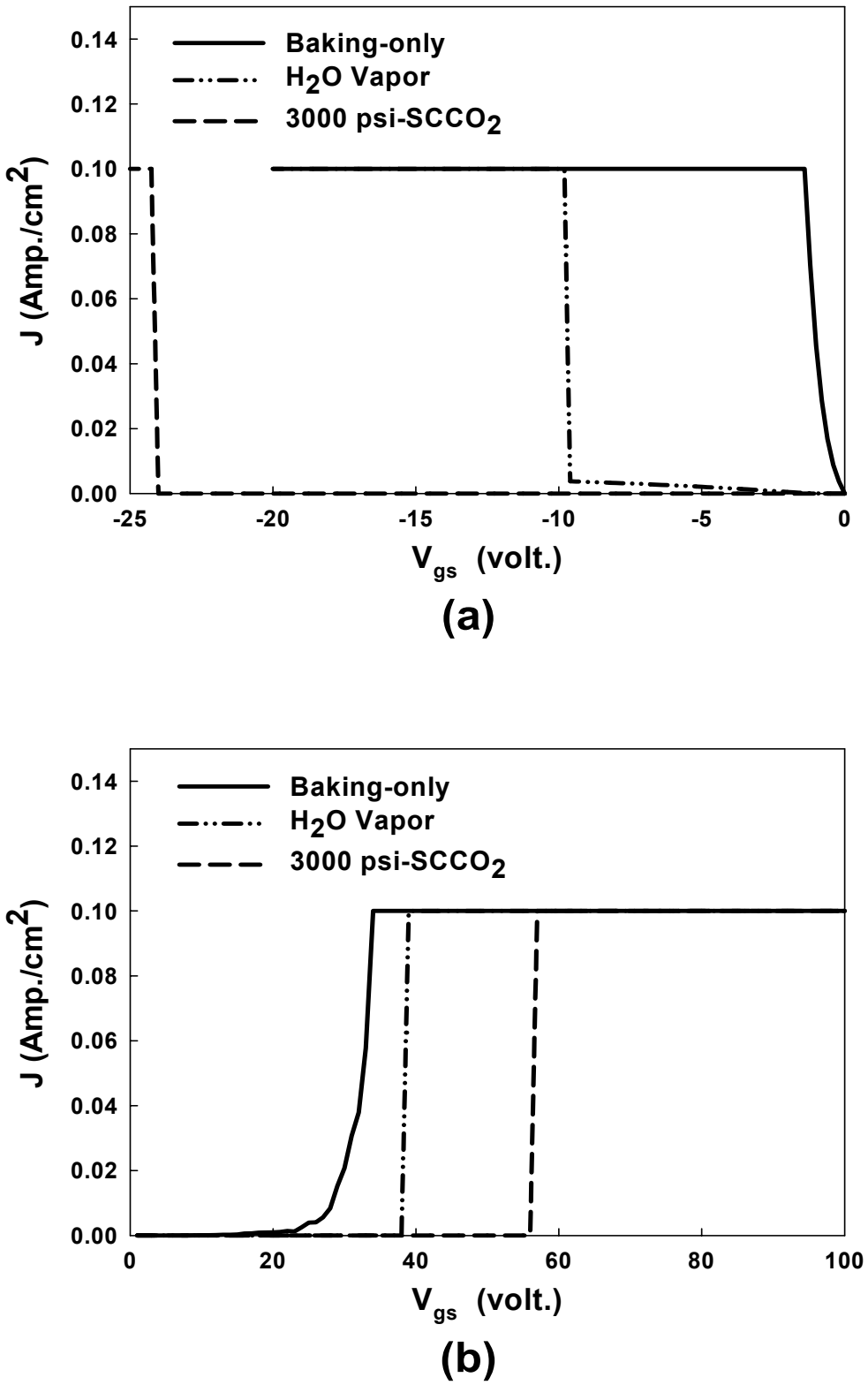

Fig. 2-19 The breakdown characteristic curves of HfO_2 films after various treatments (a) at positive and (b) at negative gate bias region, individually.

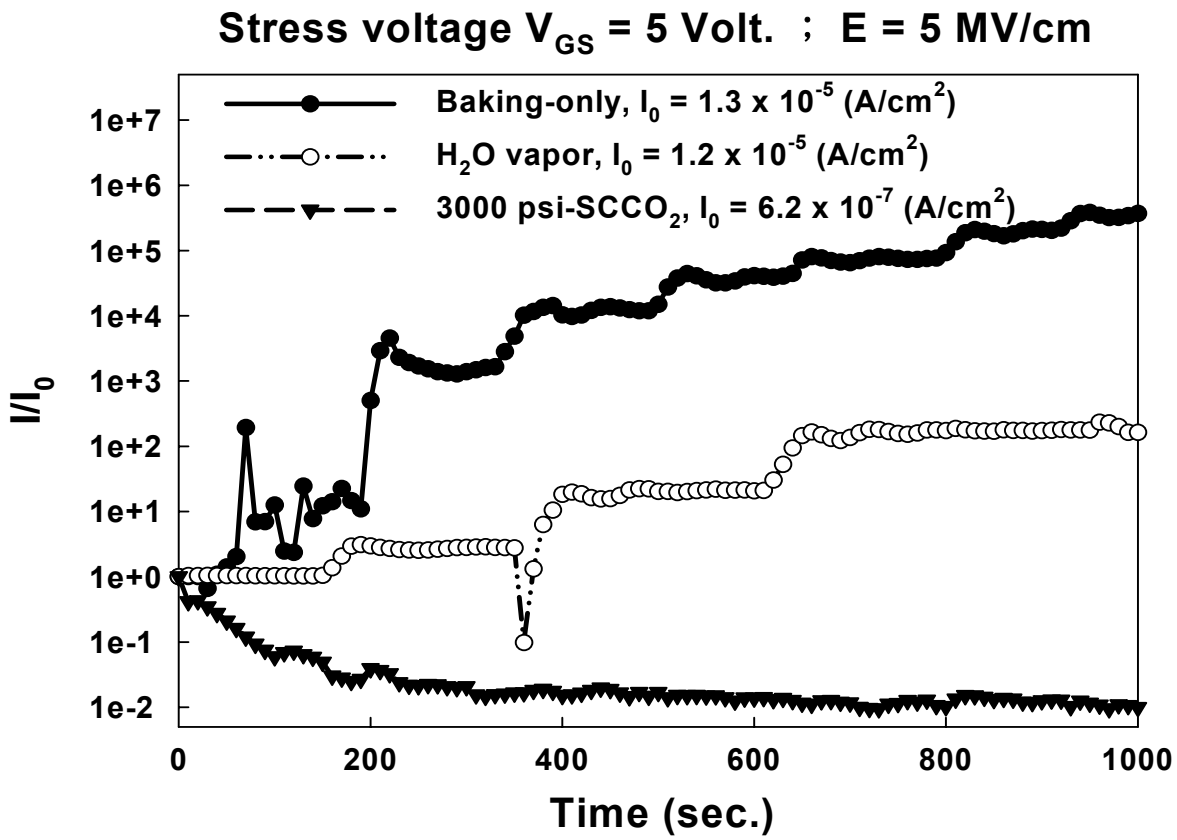

Fig. 2-20 The variation of leakage current of different-treated HfO_2 films as a function of stress time at a high electric field = 5 MV/cm.

		Bonding energy		
		Baking-only	H_2O-vapor	3000psi-$SCCO_2$
Hf 4f	Hf $4f_{7/2}$	15.88	16.03	16.37
	Hf $4f_{5/2}$	17.50	17.66	18.01

Table 2-1 Summary of binding energies for ultra thin HfO_2 films Hf 4f after various post-treatments, including Baking-only, H_2O vapor and 3000psi-$SCCO_2$ treatment.

		Bonding energy		
		Baking-only	H_2O-vapor	3000psi-$SCCO_2$
O 1S	Hf-O	530.08	530.18	530.47
	Si-O	531.50	531.64	531.83

Table 2-2 Summary of binding energies for ultra thin HfO_2 films O 1s after various post-treatments, including Baking-only, H_2O vapor and 3000psi-$SCCO_2$ treatment.

	Baking-only	H_2O vapor	$SCCO_2$-3000psi
Dielectric const.	20.4	24.8	29.4
$V_{0.5}$ (volt.), C/C_{max} = 50%	- 3.2	- 1.6	0.1
ΔV (volt.)	0.9	0.1	~ 0

Table 2-3 The extracted parameters from C-V curves of HfO_2 films after different treatment, measuring at 1M Hz with gate bias swing from negative voltage to positive voltage (forward). The V_{fb} means the flat-band voltage, and defined as C/C_{max} = 80%. The change of flat-band voltage of different- treated HfO_2 films under forward swing is label as ΔV.

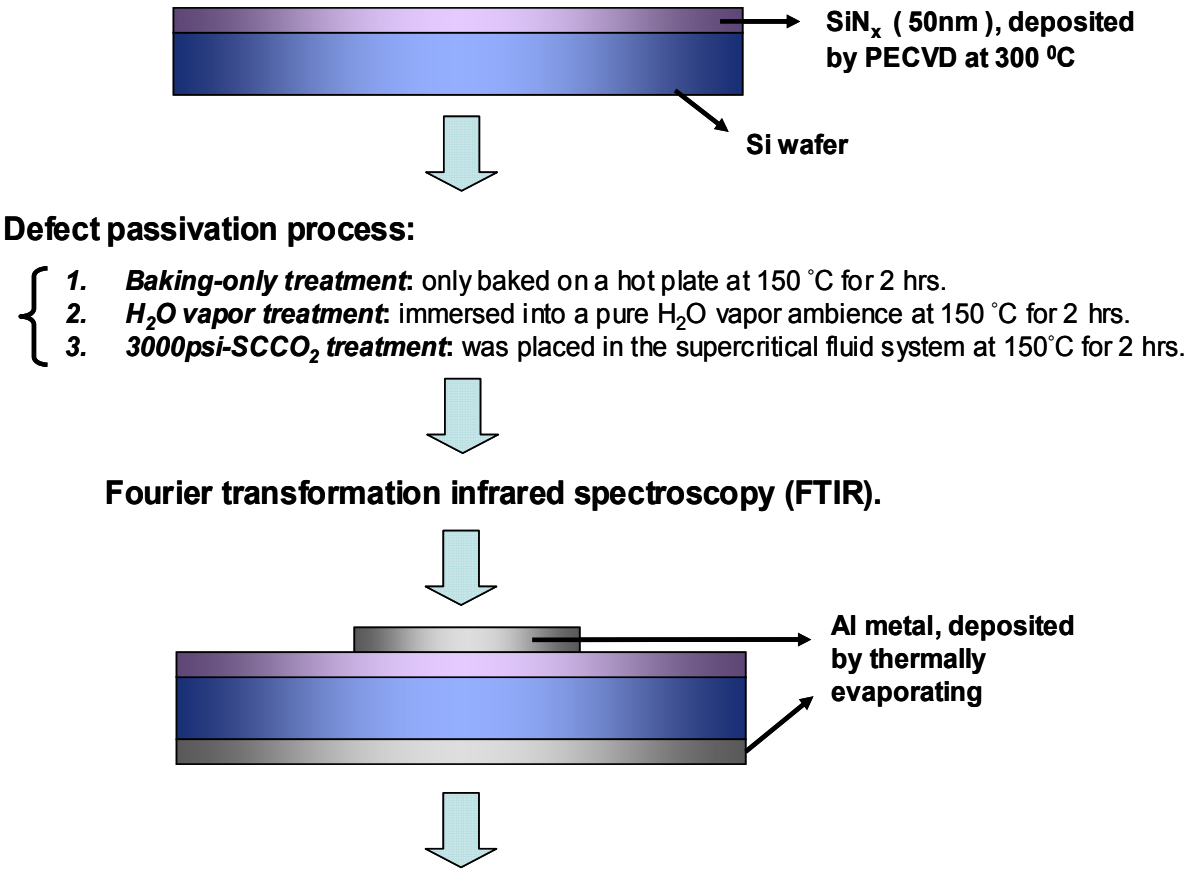

Fig. 3-1 The experiment processes of thin SiN_X film with various treatments.

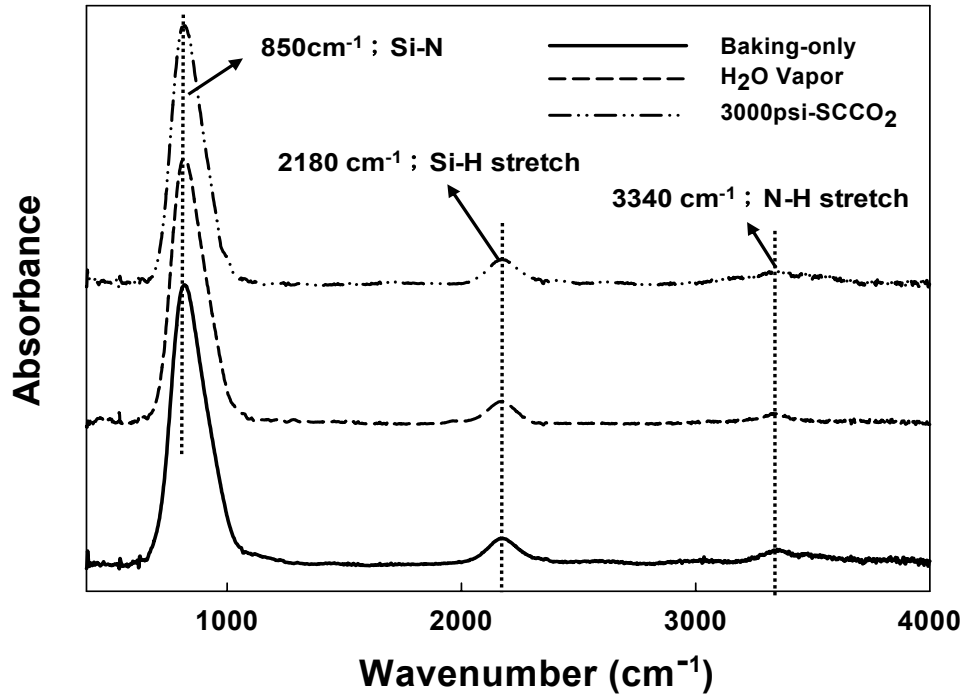

Fig. 3-2 The FTIR spectra of SiN_X films after various post-treatments, including Baking-only, H_2O vapor and 3000psi-$SCCO_2$ treatment.

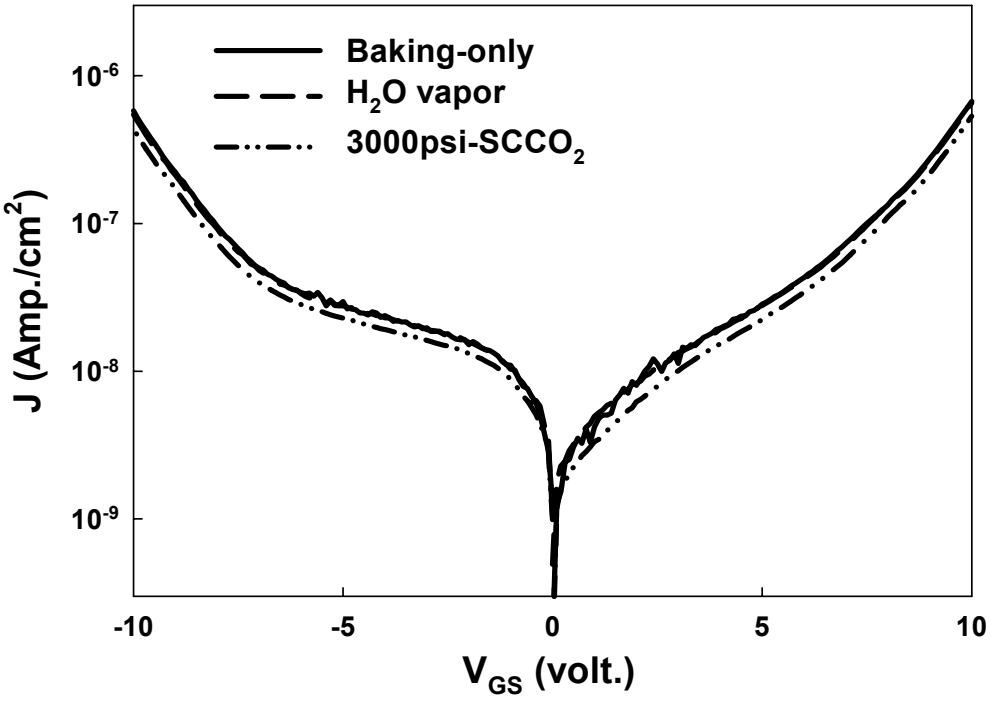

Fig. 3-3 The leakage current densities of SiN_X films after different treatments.

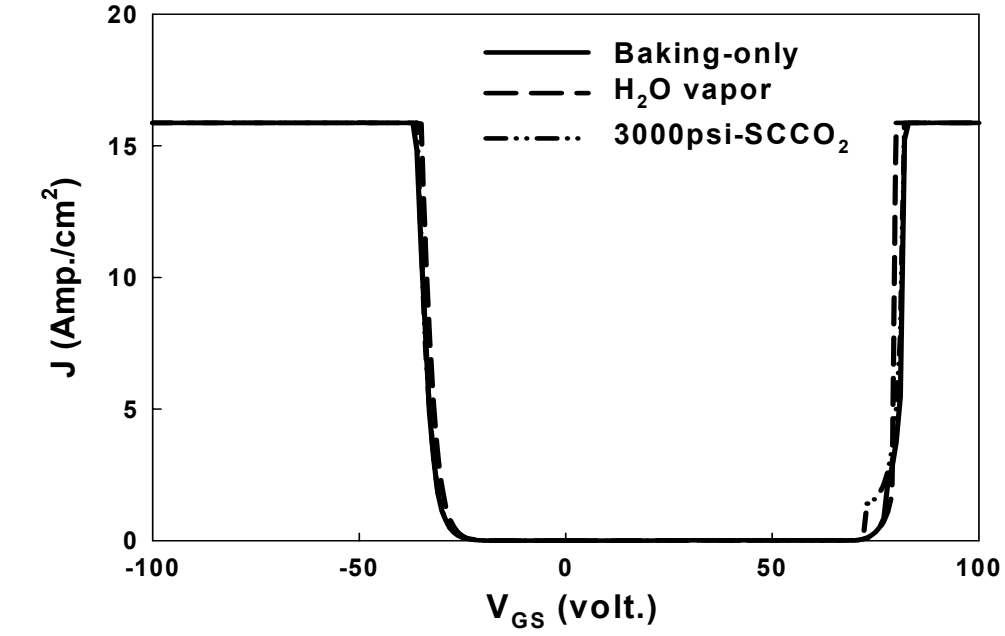

Fig. 3-4 The breakdown characteristic curves of SiN_X films after various treatments.

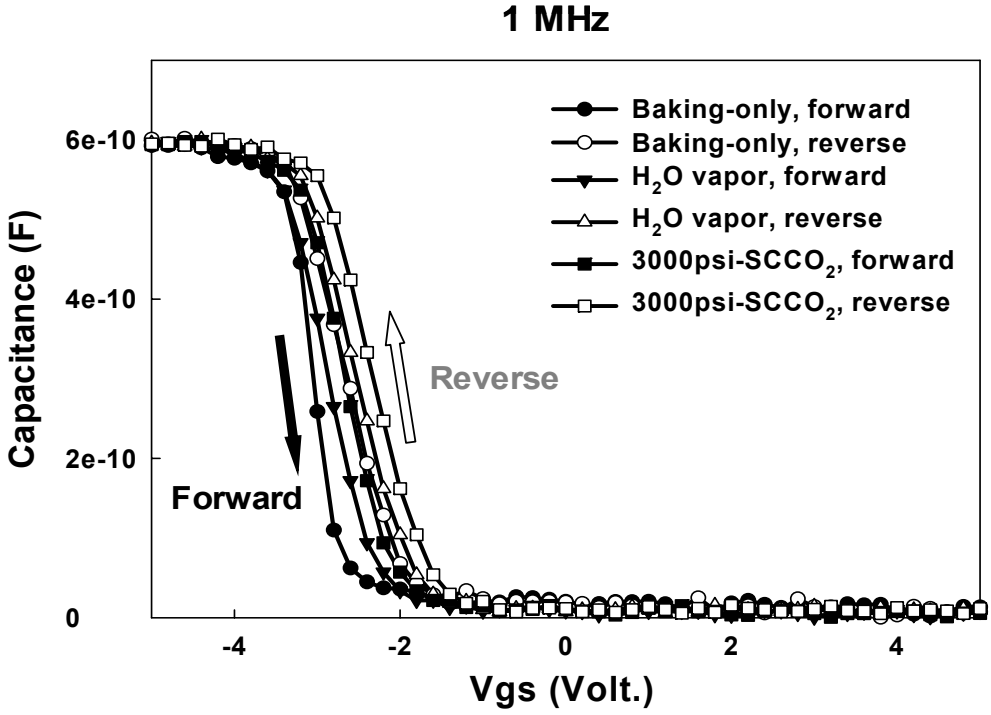

Fig. 3-5 The capacitance-voltage characteristics of SiN_X films after different treatment, measuring at 1M Hz with gate bias swing from negative voltage to positive voltage (forward) and from positive voltage to negative voltage (reverse).

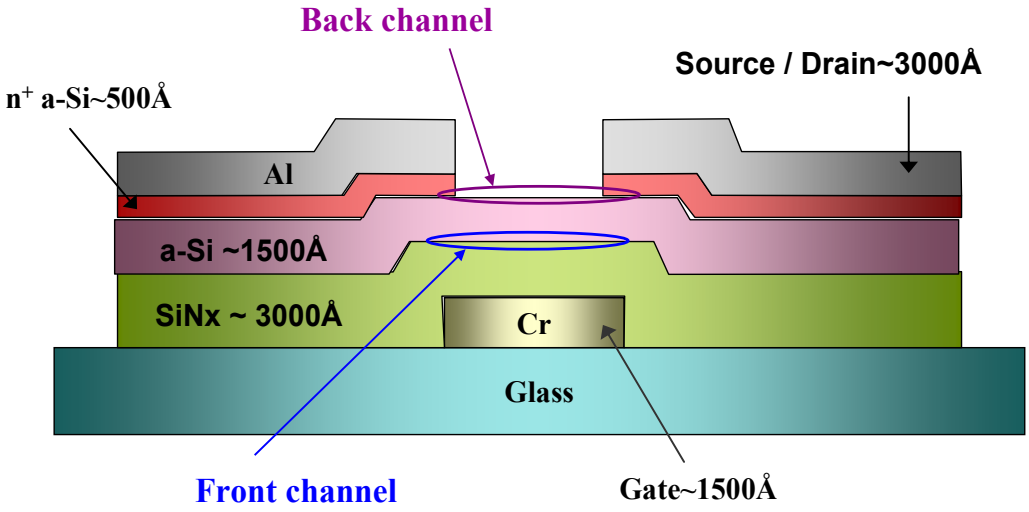

Fig. 3-6 The structure of a-Si:H TFTs.

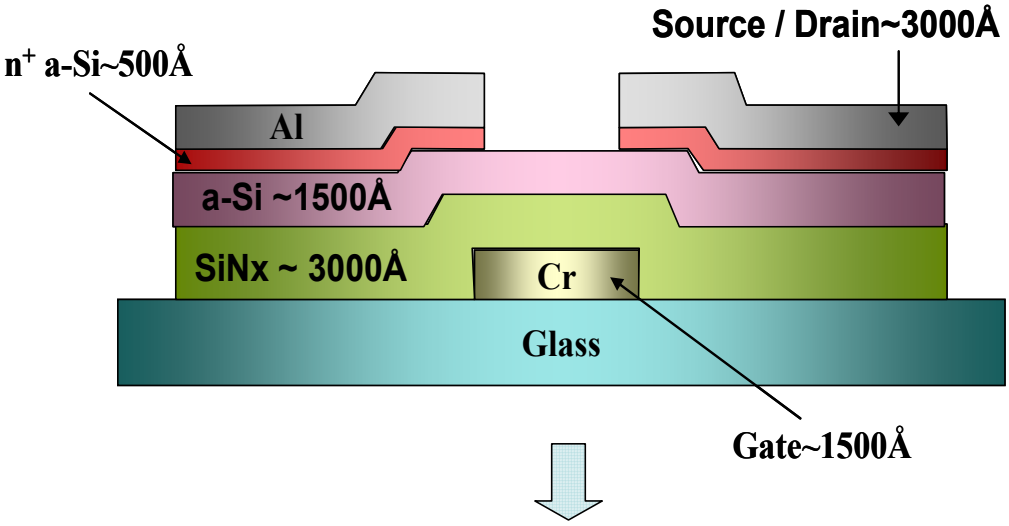

Defect passivation process:

1. ***Baking-only treatment***: only baked on a hot plate at 150 ˚C for 2 hrs.
2. ***1500~3000psi-SCCO$_2$ treatment***: was placed in the supercritical fluid system at 150˚C for 2 hrs.

Analysis of Electrical characteristics:

1. **The transfer and output characteristics of a-Si:H TFTs.**
2. **The transfer characteristics of TFT devices were measured at different temperatures (from 30 ˚C to 75 ˚C).**

Fig. 3-7 The experiment processes of a-Si:H TFTs with various treatments.

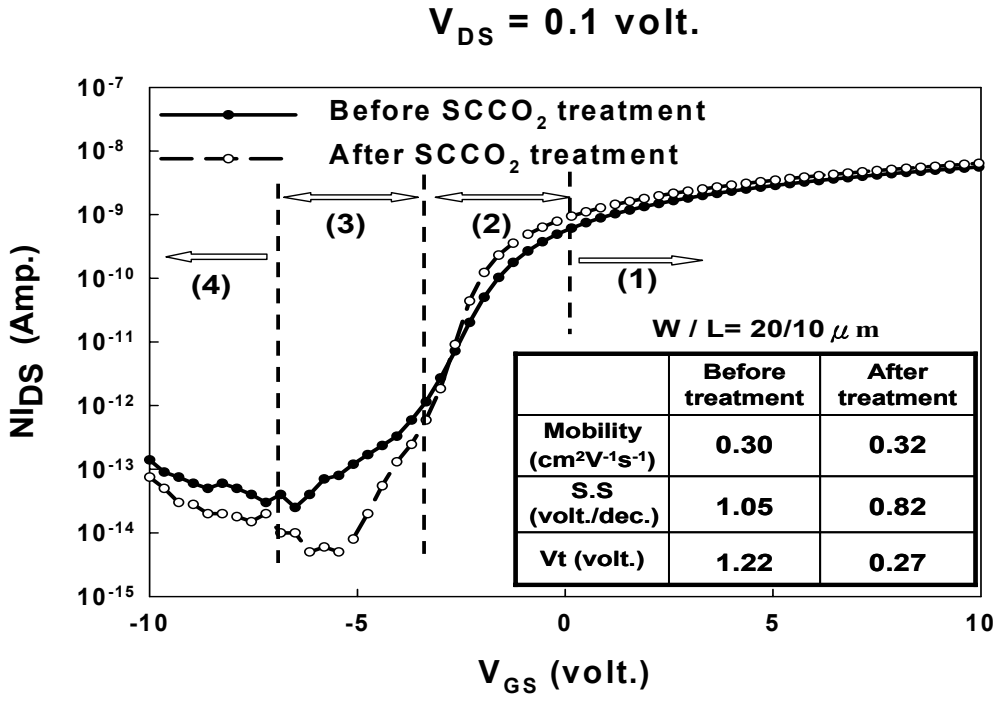

Fig. 3-8 The transfer characteristics of identical a-Si:H TFTs before and after the $SCCO_2$ treatment. The gate bias region (1), (2), (3), (4) express sequentially above- threshold, forward sub-threshold, reverse sub-threshold and Pool-Frenkel emission region [47].

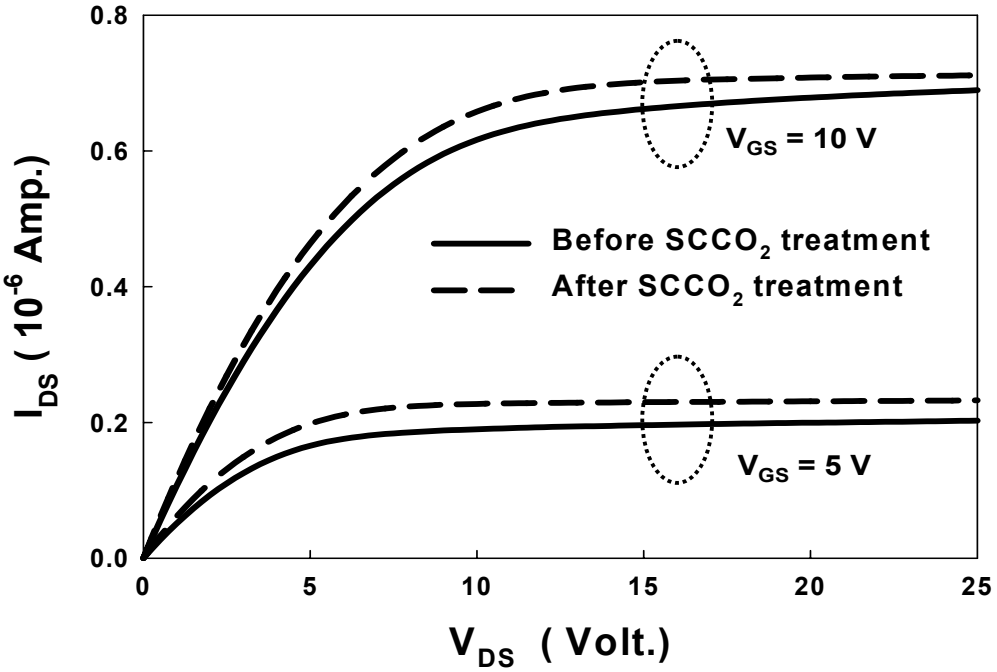

Fig. 3-9 The output characteristics of a-Si:H TFTs before and after $SCCO_2$ treatment.

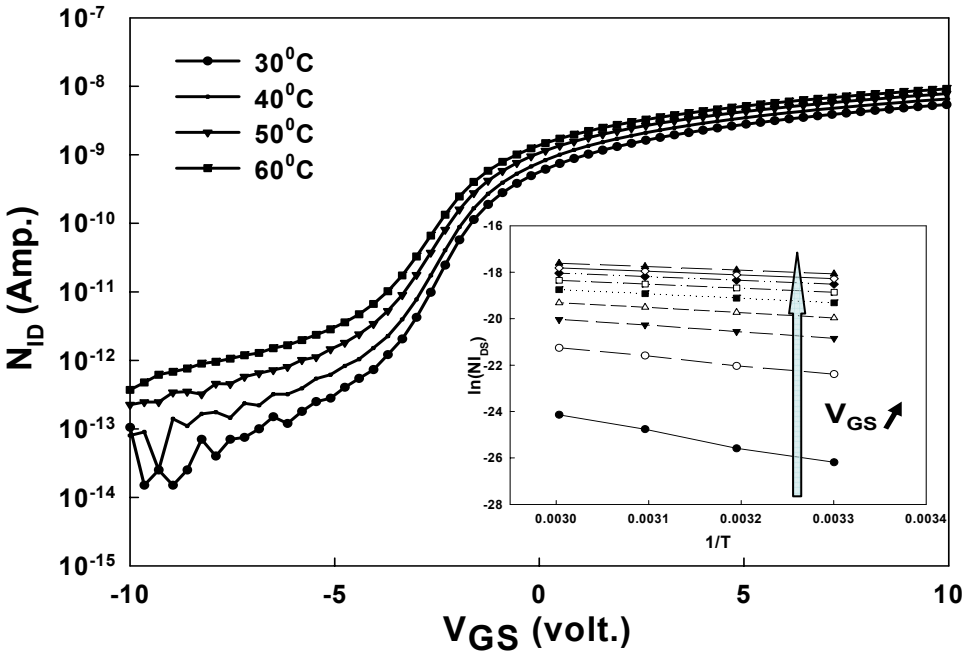

Fig. 3-10 The transfer characteristics of SCCO2-treated TFT at different temperature, in linear operation region with V_{DS} = 0.1 V. Inset is the plot of ln(I_{DS}) versus reciprocal of temperature (1/T).

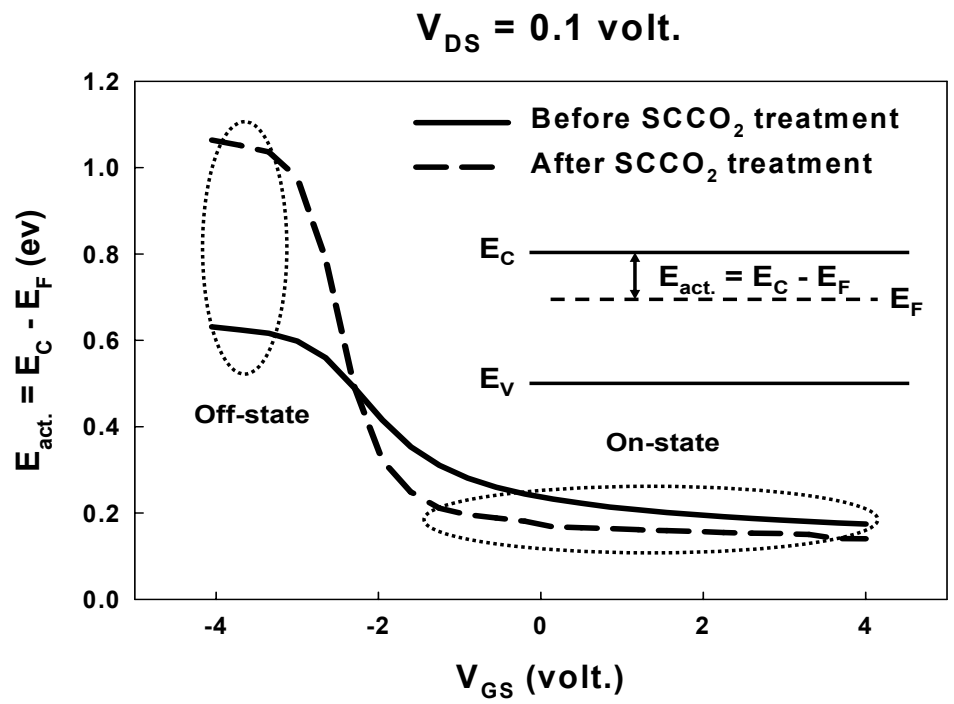

Fig. 3-11 The plot of activation energy versus gate bias, before and after $SCCO_2$ treatment. The inset shows the definition of activation energy ($E_{act.}$).

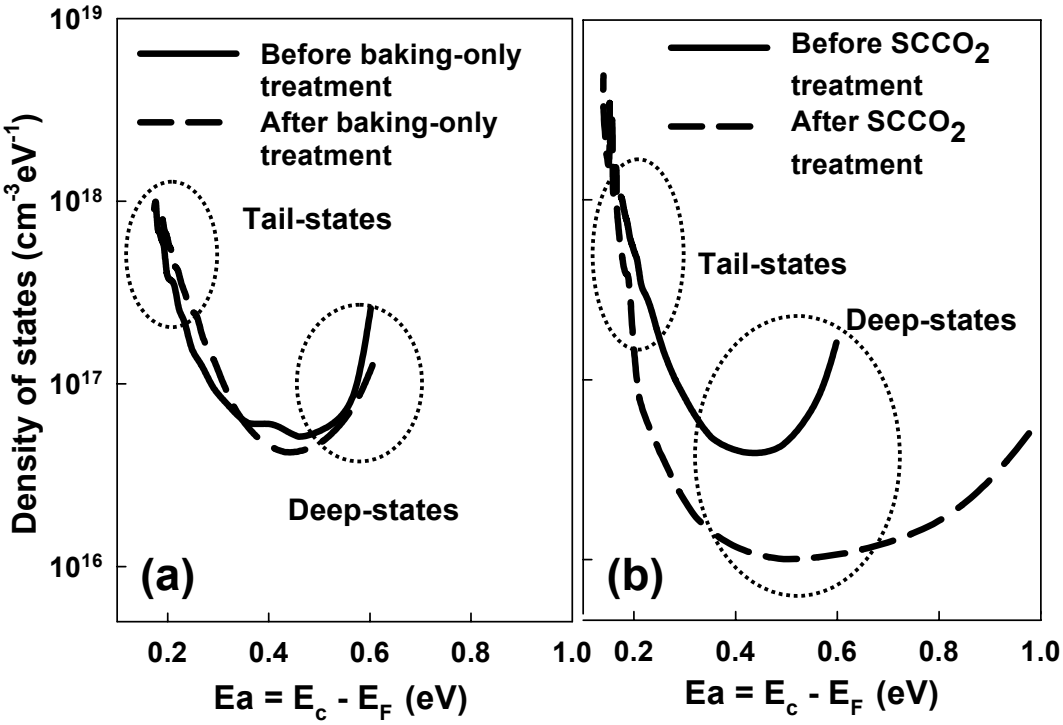

Fig. 3-12 The density of states in mobility gap of a-Si:H film. (a) a-Si:H TFT with no $SCCO_2$ treatment before and after the hot baking on a hot plate at 150 °C for 120 min, which taken as the control sample. (b) a-Si:H TFT device before and after $SCCO_2$ treatment.

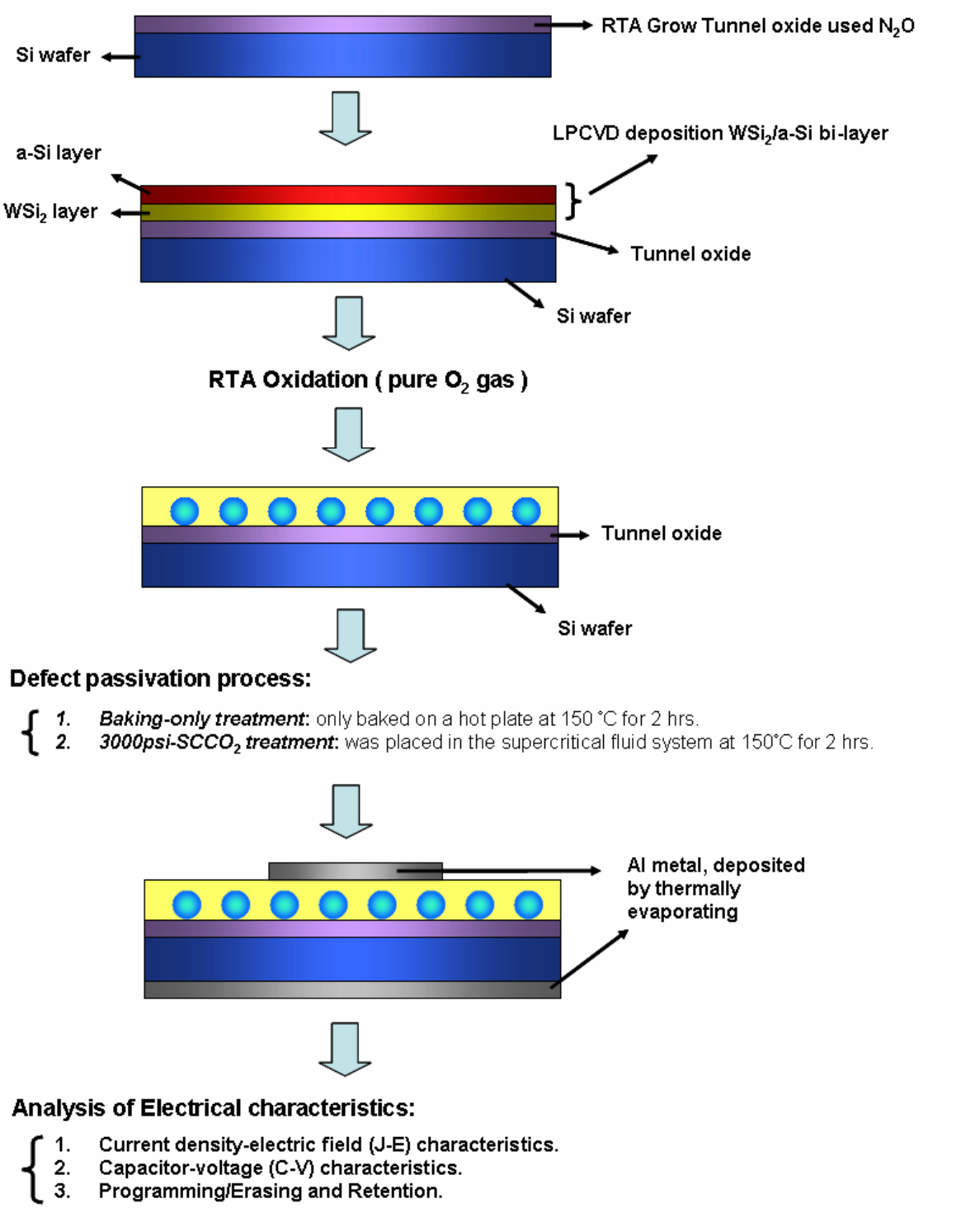

Fig. 4-1 The experiment processes of Memories with various treatments.

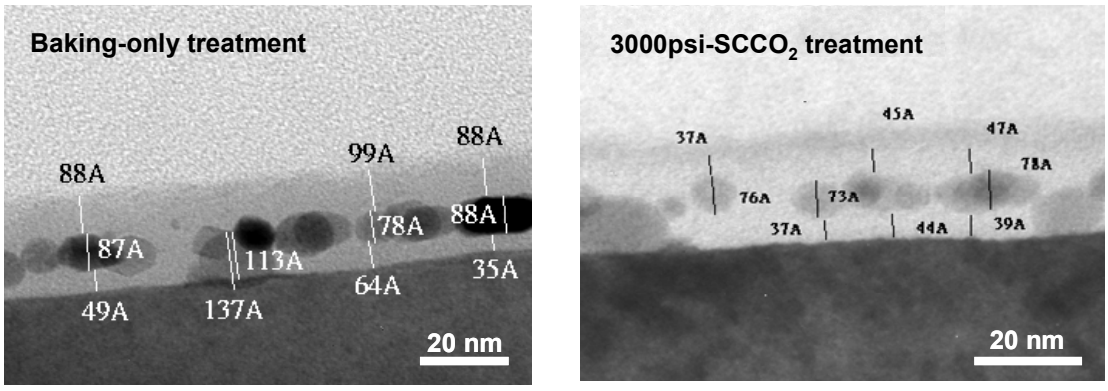

(a) (b)

Fig. 4-2 The TEM images show the Non-volatile Memories structure after various post-treatments: (a) Baking-only treatment (b) 3000psi-$SCCO_2$ treatment.

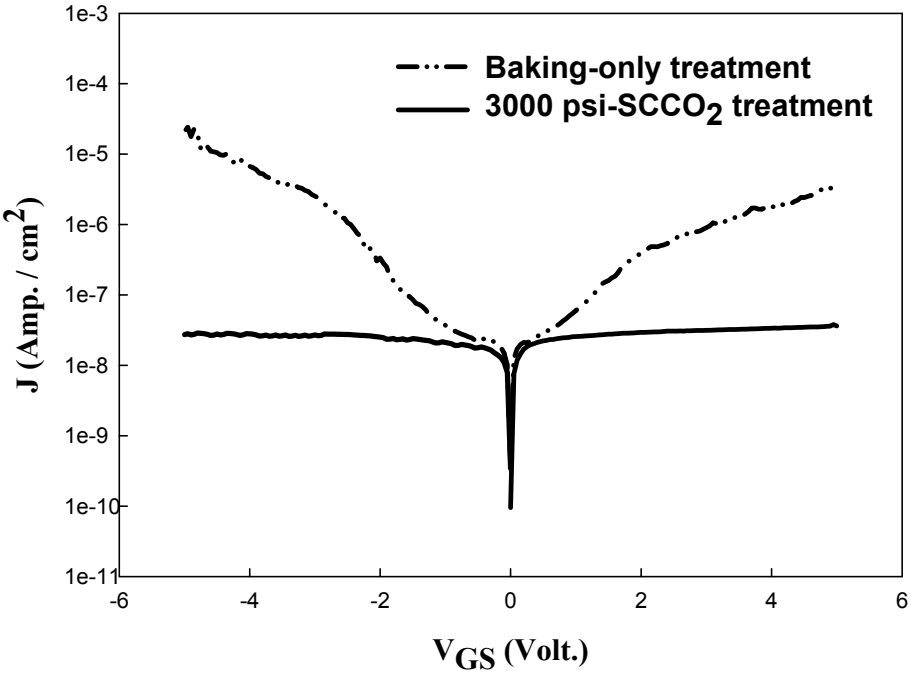

Fig. 4-3 The leakage current densities of Non-volatile Memories after different treatments.

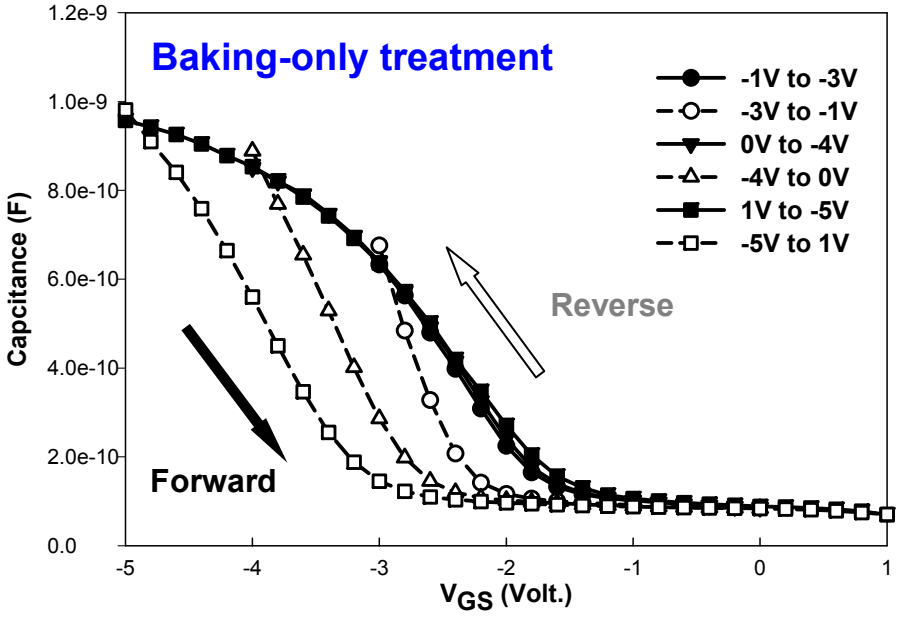

(a)

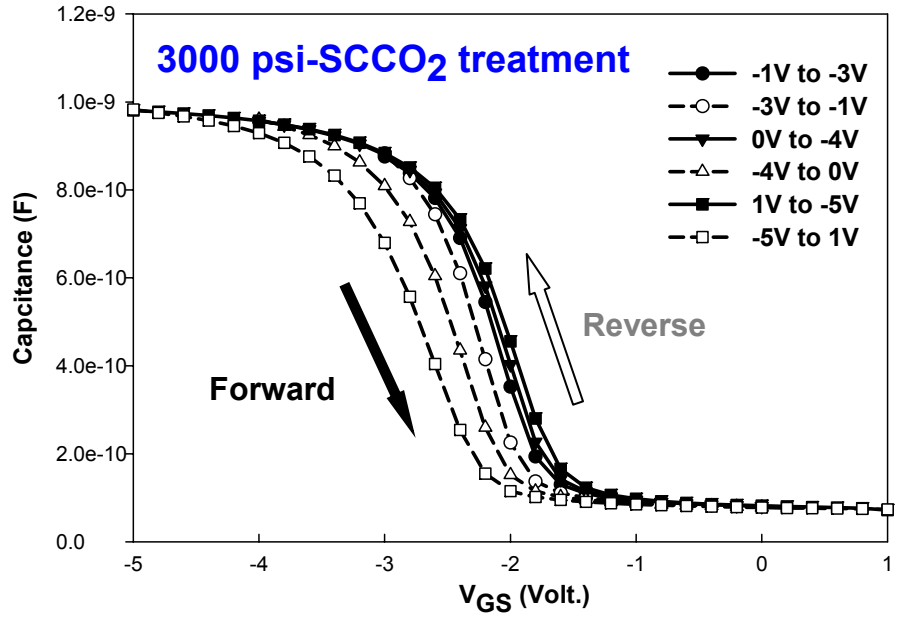

(b)

Fig. 4-4 The capacitance-voltage hysteresis characteristics of Non-volatile Memories after different treatment: (a) Baking-only treatment (b) 3000psi-$SCCO_2$ treatment.

.

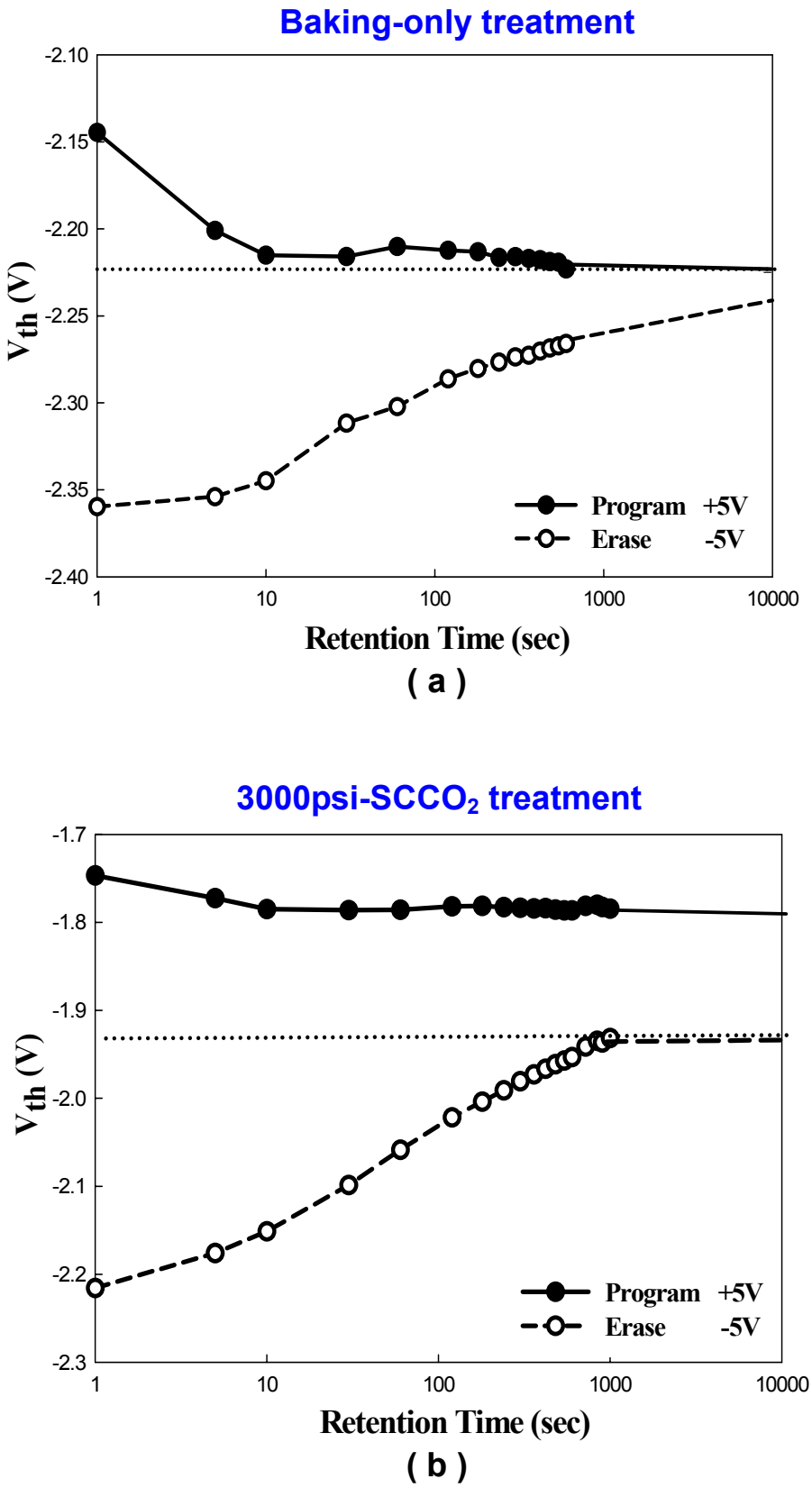

Fig. 4-5 The retention characteristics of Non-volatile Memories after different treatment: (a) Baking-only treatment (b) 3000psi-$SCCO_2$ treatment.

	Baking-only treatment	3000psi-$SCCO_2$ treatment
Program / Erase (V)	P(+5V) / E(-5V)	P(+5V) / E(-5V)
Decay Rate 1~1000 (mV/dec)		-12.5
Retention 20% Time (Sec)	< 5	9.32E+04

Table 4-1 Summary of electrical Characteristics for Non-volatile Memories after various post-treatments, including Baking-only and 3000psi-$SCCO_2$ treatment.